1135

RESEARCH AND DEVELOPMENT REPORT
REPORT 1135
4 SEPTEMBER 1962

NEL/Report 1135

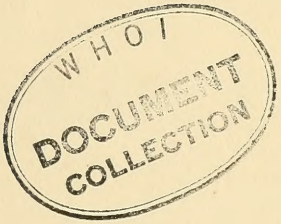

MEASUREMENT OF ATTENUATION OF LOW-FREQUENCY SOUND (5-8 KC/S) IN SMALL SAMPLES OF SEA WATER

P. G. Hansen

U. S. NAVY ELECTRONICS LABORATORY, SAN DIEGO, CALIFORNIA
A BUREAU OF SHIPS LABORATORY

TK
7855
.U5
no. 1135

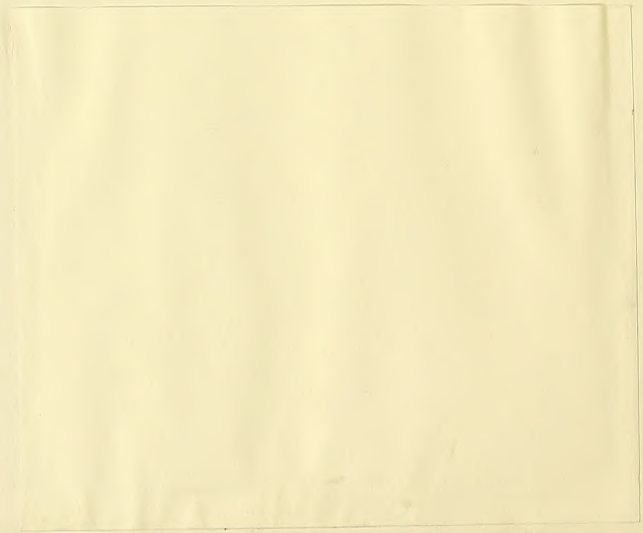

THE PROBLEM

Develop equipment for measuring the sound attenuation at low frequencies in small samples of sea water. The attending disturbance of the sample from its natural state should be kept as low as possible.

Correlate the results with other oceanographic variables and explain the correlations obtained.

RESULTS

1. Equipment which utilizes cavity resonators with acoustically soft side walls was developed. The effects of wall contamination on the measurements are therefore kept to a minimum. The attenuation can be measured at discrete frequencies between 5 and 8 kc/s, provided it falls in the range from 10 to 200 db/kyd.

2. Natural sea water with suspended particulate matter and high oxygen content showed attenuations in the whole range the equipment was capable of measuring (10-200 db/kyd). Sea water free of particulate matter never showed any measurable attenuation. The attenuation of clean sea water is about 0.5 db/kyd at 5000 c/s, and this is below the lower limit set by the equipment. It is suggested that the excess attenuation may be explained by the presence of a large number of very fine bubbles or bubble nuclei.

RECOMMENDATIONS

1. Include an investigation of small bubbles and nuclei in future work. Give special attention to plankton, since air spaces inside a living cell will have an especially marked effect due to the surrounding organic matter. Use cavity

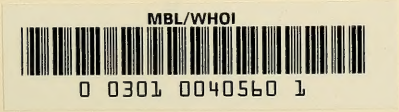

methods for this work, since the effect of a single bubble or a small quantity of plankton then can be determined.

2. Raise pure cultures of living plankton in the laboratory to ascertain the effect of living plankton and dead organic matter separately.

ADMINISTRATIVE INFORMATION

Work was begun under SR 004 03 01 (NEL L4-1) and S-F011 02 09 (NEL L1-7) and completed under the new problem designation SR 004 03 01, task 0580 (NEL L4-4). The manuscript was completed in January 1962 and submitted to the Graduate School of the Agricultural and Mechanical College of Texas in partial fulfillment of the requirements for the degree of Doctor of Philosophy. This report is a slightly modified version of the doctoral dissertation. It covers work from March 1959 to November 1961 and was approved for publication 4 September 1962.

The author is especially indebted to:

Dr. G. H. Curl for the discussions and advice during the period of the investigation, and his reading and criticism of the manuscript.

Dr. E. C. LaFond for his interest and support during the measurement phase and his assistance in the procurement of necessary equipment and facilities.

Dr. E. G. Barham for his assistance with the phases of marine biology involved.

Professor R. O. Reid, my committee chairman, for his help and advice with the theoretical parts, as well as help and guidance with the editing of the dissertation.

Mr. S. A. Burnett for his interested and skillful help in changing ideas into hardware during the development of the cavities and transducers utilized in the project.

CONTENTS

LIST OF SYMBOLS USED IN TEXT...*page iv*
I. INTRODUCTION... *1*
II. METHODS OF MEASUREMENT... *3*
Field Methods... *3*
Laboratory Methods: Plane Wave Propagation... *4*
Laboratory Methods: Three-Dimensional Wave Propagation... *6*
Soft Wall Cavity Resonators... *8*
Influence of Air Bubbles... *9*
III. DESIGN CONSIDERATIONS... *11*
Cylindrical and Spherical Cavities... *11*
Box-Shape Cavities... *13*
IV. THEORETICAL DISCUSSION... *25*
Acoustical Wave Equation for Viscous Fluids... *26*
Some Special Solutions of the Wave Equation... *41*
V. EXPERIMENTAL PROGRAM... *60*
Observational Platform... *60*
Experimental Procedure... *62*
Discussion of Results... *73*
VI. SUMMARY AND CONCLUSIONS... *97*
Primary Results... *97*
Suggestions for Future Studies... *98*
REFERENCES... *101*

ILLUSTRATIONS

1-2 Schematics of preliminary and final cavity designs...*page 15*
3 Sound transducers (preliminary and final models)... *17*
4 Diagrams of measuring systems... *19*
5-7 Reverberation curves obtained with Brüel and Kjaer recorder... *21-23*
8 Photograph of data-collecting equipment... *24*
9-14 Calibration data recorded under various conditions... *67-69*
15 Reverberation curves using data of figures 5, 6, and 7... *71*
16-32 Attenuation values as determined from measurements on sea water samples under various conditions... *77-86*

LIST OF SYMBOLS USED IN TEXT

A	Surface area; A_i amplitude parameters.
B	Arbitrary constant.
b	Coefficient of thermal expansion (volumetric).
C_p	Specific heat at constant pressure.
c	Sound speed $(\lambda_o / \rho_o)^{\frac{1}{2}}$.
c^*	Complex sound speed.
D	Clearance between free surface and top of cavity (figure 9).
D_{ik}	Deformation (strain) tensor ($i = 1, 2, 3$; $k = 1, 2, 3$).
E	Acoustic energy (intrinsic plus kinetic).
e	Base of natural logarithms.
$\hat{F}$	Body force.
f	Frequency (c/s); or functional notation.
i	Integer suffix ($i = 1, 2, 3$).
j	Unit imaginary number.
K	Isothermal compressibility coefficient.
K_t	Thermal conductivity coefficient.
K_i	Complex wave number corresponding to coordinate x_i.
k	Integer suffix ($k = 1, 2, 3$) independent of i.
k_i	Real part of wave number.
ℓ_i	Dimensions of rectangular cavity resonator.
L	Gross scale factor (volume/surface area).
m	Mass per unit area of flexible wall.
n	Unit normal to boundary (the components n_k being the direction cosines of the boundary).
n_i	Integer designating the mode of oscillation.

P	Pressure.
p	Acoustic pressure (anomaly from hydrostatic value of P).
Q	Quality factor (see page 11).
r	Resistive (real) part of boundary impedance Z; also bubble radius (page 90 only).
S	Bounding surface.
$\hat{s}$	Particle displacement vector (components s_i).
T	Absolute temperature (T_0 mean value, T_1 anomaly from mean value); also surface tension (page 90 only).
t	Time
t_0	Reverberation time for cavity with pure water.
t_{total}	Reverberation time for cavity with sample sea water.
$\hat{v}$	Fluid velocity vector (components v_i).
v	Magnitude of velocity vector ($v^2 = v_1^2 + v_2^2 + v_3^2$).
V	Volume.
x_i	Components in a Cartesian coordinate system ($i = 1, 2, 3$).
Z	Boundary impedance (Z_i and Z'_i, $i = 1, 2, 3$ correspond to values pertinent to the six faces of a rectangular cavity resonator).
α_i	Spatial (or range) coefficients of attenuation (db/kyd).
α_t	Temporal coefficient of attenuation (db/sec); see page 57 for special designation.
β	Parameter controlling viscous loss, $(2\mu_1 + \lambda_1)/\lambda_0$.
γ	Transmission coefficient for energy flux.
ΔL	Effective thickness of walls (m/ρ_0).
δ_{ik}	Unit diagonal tensor; unity for $i = k$, zero for $i \neq k$.
η	Anomaly of specific entropy from equilibrium value (ergs/gm °K).
Θ	Dilation, $\nabla \cdot \hat{s}$.
$\varkappa$	Thermal diffusivity.

λ_o	Second Lame parameter.
λ_1	Second viscosity coefficient.
μ_o	First Lame parameter.
μ_1	First viscosity coefficient.
π	3.14159 ...
ρ	Density; ρ_o is mean density.
σ	Element of surface area.
τ_{ik}	Total stress tensor (normal components being tensile stresses if positive).
ψ	Phase parameter.
Ω	Complex frequency.
ω	Real frequency (radians/sec).
∇	Gradient operator.
$\prod$	Standard symbol for repeated multiplication.
$\sum$	Standard summation notation.

I. INTRODUCTION

It is well known that the propagational characteristics of acoustical energy depend upon the type of material medium and the distribution of inhomogeneities within the medium. An abrupt change in the ocean medium as occurs at the sea surface or sea bed produces reflection or reverberation of acoustical energy. Variations of sound speed in the sea produce refraction effects. The presence of air bubbles or suspended material, including plankton, will produce scattering of the sound energy. Viscosity, diffusion, certain thermochemical effects, and other non-reversible processes can lead to absorption of sound energy.

The biota of the sea can also influence the acoustic properties to a marked degree. Schools of fish not only can give rise to echoes, but can also impair the transmission of a sonic beam of energy from point to point by scattering the energy out of the beam. The best known effect of this sort is perhaps the deep scattering layer. It appears on a fathometer record as a false bottom above the true bottom and in view of its vertical migration during the day, is thought to be caused by a layer of organisms.

In recent years there has been an interest in the properties of low-frequency acoustic energy in the sea. Theoretically, the viscous attenuation coefficient of acoustic energy in a plane sound wave is directly proportional to the square of the frequency. However, in view of other sources of attenuation, particularly the scattering and absorption associated with air bubbles and plankton, it is expected that anomalous attenuation can occur. The present report is concerned with the problem of isolating some of the factors producing attenuation of low-frequency acoustic energy in sea water.

Several of the above mentioned inhomogeneities of the medium are almost always present at the same time. This makes it difficult in field measurements to separate the different effects of temperature and salinity gradients,

fish, plankton, and properties of surface and bottom. It is therefore desirable to employ a measurement technique that requires a relatively small sample when studying the medium since difficulties from inhomogeneities then can be avoided, and cause and effect can be established. It is also desirable to be able to undertake the measurements as soon after sampling as possible, to keep changes in the water at a minimum. The first requirement was met by using a soft or compliant wall cavity method developed at the U. S. Navy Electronics Laboratory, and the second requirement was satisfied by using NEL's oceanographic tower off Mission Beach, San Diego, California, as the supporting operations facility.

II. METHODS OF MEASUREMENT

A great amount of work on the determination of sound absorption in liquids exists in the literature and it is clearly necessary to limit the discussion of methods of measurement to those aspects which are most pertinent to the present investigation--specifically, the influence of biological entities and air bubbles on sound propagation in sea water and the methods of measuring them. The references cited here have been chosen with the aim of presenting a representative cross section of the recent work in this field. There exist several articles and texts covering the broad aspects of the problem of sound attenuation.[1-4] (See list of references at end of report.)

Attenuation can be measured by (1) field methods, taking place in the ocean where the disturbance of the sample can be kept at a minimum; and (2) laboratory methods, which involve taking samples out of the ocean to perform the measurements.

FIELD METHODS

The direct(and the simplest)method consists of introducing two hydrophones in the ocean and performing transmission measurements. The inherent difficulty is that the measurements are influenced by a large number of variables, and it is difficult to unscramble the combined effects so as to achieve dependable conclusions about the influence of the plankton population.

For clear sea water the attenuation is small and it is therefore necessary to use long distances between transmitting and receiving hydrophones. Moreover, the influence of thermal stratification and of reflections and losses at surface and bottom, as well as the intensity changes due to spreading of the acoustical beam, must be accurately known. The direct method has been used to determine the

sound velocity, and it has also demonstrated that the attenuation in sea water is extremely small, when the water is free of contamination. By way of illustration, Horton* states that the attenuation coefficient in pure sea water is approximately 0.5 db/kyd at 5000 c/s.

Studies carried out by the direct method[5-7] clearly demonstrate the difficulties involved. Chief among these difficulties is that of assessing the influence of plankton. Plankton is far from homogeneously dispersed in the ocean. It occurs frequently in quite sharply defined layers, and is often very patchy within the layer. To determine the acoustic attenuation by plankton from an interpretation of measurements obtained by the direct method is therefore virtually impossible and has not been attempted.

A few methods classified here as laboratory procedures have been modified for field use. A method of velocity measurement by spherically propagating sound waves has been adapted for field measurements.[8] However, in this system, the path length involved is too short for obtaining any useful information about attenuation. Adaptation of the reverberation tank to field use is more pertinent to the attenuation problem.[9]

The direct field methods have served mainly in identifying certain propagation anomalies in a gross sense and in emphasizing the need for more detailed studies. Such anomalies as the deep scattering layer, effect of ships' wakes, "quenched water," "knuckles," and "black-outs"** have been detected by direct methods.

LABORATORY METHODS: PLANE WAVE PROPAGATION

Laboratory methods require only a relatively small liquid sample and therefore lend themselves to measurements of the acoustic properties of more or less exotic

---

*Ref. 1, p. 81

**Ref. 1, p. 82

liquids of high purity, which can be obtained only in relatively small quantities. Such measurements are of great interest to the physicist, since they offer one of many useful approaches to the investigation of the nature of matter.

The laboratory methods divide naturally into two groups. The first utilizes one-dimensional (plane wave) propagation, and the second utilizes three-dimensional wave propagation.

The instruments belonging in the first group include acoustic interferometers, and equipment resembling interferometers, but utilizing pulsed rather than continuous signals. Plane waves are usually obtained by using transducers with a flat actuating surface, large compared with the wavelength of the sound. For this purpose a quartz crystal is usually employed, especially for the high-frequency acoustic waves.

Interferometers measure the sound velocity by utilizing a reflector and create a one-dimensional standing wave system. A change in the distance between reflector and transmitter by an integral number of half-wavelengths will not disturb the standing wave pattern. The sound velocity can therefore be determined from the frequency and the half-wavelength. The detection of the standing wave pattern can be done by one of several methods: (a) measurement of the drive current to the transmitting crystal at constant voltage, (b) employment of a second crystal as a reflector and also as a receiver, and (c) utilization of a suitable optical system.[10-12]

The sound velocity can also be evaluated by impressing pulses of the desired frequency on the transducer and measuring the time of flight from transmitting to receiving crystal.[13] A transistorized version of a pulsed interferometer is being used for sound velocity measurements in the field.[14]

Both types of equipment (those using continuous and pulse signals) are also suited for attenuation measurements,

but only when the measuring frequency is high. The main limitation is that the sound beam must be long enough to cause a reasonable amount of attenuation. This places a practical restriction on attenuation measurements with this equipment to frequencies above 1 Mc/s.[15]

Plane waves can also be obtained by letting the wave propagation take place inside a tube of a material with a much higher specific acoustic impedance than the fluid under investigation. This requirement can be met easily for gases, since ρc of steel is about 10^5 times larger than ρc of air (ρ being the density of material and c the sound speed). The same ratio for steel and water, however, is only about 25.

Tube interferometers have nevertheless been successfully used on liquids and mixtures of liquids with water as the main constituent, but only under special circumstances.[16-19] These methods would not be suitable in the present problem, since the attenuation in many cases is too small to allow the utilization of a tube of reasonable length. Furthermore a difficulty is encountered in the presence of air bubbles on the wall. This is the same difficulty explained later under resonating cavities. In the case of fluids which contain a high density of bubbles within the fluid itself, the presence of the bubbles may actually enhance the use of the tube interferometer since the acoustic impedance of the fluid is thereby lowered while the absorption coefficient is increased.[19]

LABORATORY METHODS: THREE-DIMENSIONAL WAVE PROPAGATION

There are two subgroups in this division: reverberant chambers and resonant chambers. The reverberation methods all utilize a "diffuse" sound field, i.e., a very large number of normal modes are energized at the same time, and these modes must be close together in frequency. The volume of the sample required is therefore quite large,

if measurements at low frequencies are desired. The containers should not be of too regular shape, in order to insure a "diffuse" sound field with minimum volume of sample. Spheres, as used by Moen,[20] and cubes have too many degenerate modes to be well suited. Bubbles settling down on the walls may actually be helpful under special circumstances by coupling different modes together.

In contrast to the reverberant chambers, the resonant cavity involves the excitation of a pure normal mode, characteristic of the particular cavity shape and size. The resonant cavity method is the only practical method that permits attenuation measurements at low frequencies on relatively small samples.

The reverberant chamber method was employed by Knudsen for air-acoustic investigations.[21] It has been extended for use with water by Leonard, and by Wilson and Liebermann. Mulders used the method near 1 Mc/s, and needed 2 to 3 liters of liquids for the measurement.[22] The smallest absorption he could measure was of the order of 100 db/kyd. Moen[20] employed bottles of spherical shape ranging from 1 to 12 liter capacity for attenuation measurements of water. The smallest frequency investigated by Moen was 140 kc/s.

Glotov[9] has suggested a reverberation method for use in the field. The volume of sea water required is 500 liters, and the lowest frequency utilized is 15 kc/s. Clearly it would be difficult to obtain homogeneous plankton samples of such large size, even though it is quite possible to utilize this type of equipment to measure the sound attenuation in natural sea water. Glotov indicates that even for this type of equipment, the bubbles on the walls pose a problem, since the equipment has to be conditioned at a depth of 60 meters before every measurement.

There are essentially two types of resonant chambers: the hard wall cavity and the soft wall cavity. The hard wall cavity has been employed extensively for determining

sound attenuation in pure liquids at low frequencies. The shape of the container is almost always spherical, since this shape eliminates losses due to shear at the boundary for the radial modes. The slightest contamination of the cavity wall, however, will upset the results, and it is hardly possible to get reliable measurements with anything but carefully purified and degassed liquids. A development of the theory for the spherical resonator can be found in reference 23. The practical application of this method is demonstrated in references 11, 24, and 25.

Since a few bubbles on the hard wall will completely negate the results, it is virtually impossible to use this method for natural sea water, where the measurements must be performed rapidly and cleaning must be relatively easy. The most promising solution for sea water appears to be the use of soft wall cavities. The surface of water is an excellent reflector of sound waves, and a small bubble trapped in the surface film will have no effect on the reflection of sound. Making a box-shaped cavity of thin sheet stock will give almost complete pressure release at the boundaries, since very little force is required to bend the thin metal sheet. A bubble attached to the boundary will therefore have only a minor effect.

SOFT WALL CAVITY RESONATORS

Soft wall cavities were first constructed by W. J. Toulis at the Navy Electronics Laboratory in the summer of 1953, and the best available in 1957 had a Q factor of approximately 2000 at a frequency of 5 kc/s. This implies a reverberation time* of approximately 0.9 second. This method was considered very promising for the present investigation. Furthermore, some equipment of this type was already available, so a development program of this method was undertaken, as described in the preceding section.

---

*The reverberation time is the time in seconds it takes the sound intensity in a cavity to diminish 60 db.

In order to gain a better understanding of the soft wall cavity an attempt has been made in section IV to develop a foundation for the theory describing some of the basic characteristics of the system. An approach to this problem had been made by Toulis.[26] The theory developed in section IV follows the procedure for room acoustic theory discussed by Hunt,[27,28], Morse,[29] and Morse and Bolt.[30] However, it was necessary to employ the wave equation for a viscous medium. In this connection the phenomenological approach suggested by Markham, et. al.* and Skudrzyk** served as a guide.

The wave equation utilized in section IV considers the first and second coefficients of viscosity as independent. The question of the relationship between the first and second coefficient of viscosity has been much debated since Stokes' original paper on this problem[31] and it cannot be claimed to be fully resolved.[12,32] This question, although pertinent to the quantitative evaluation of the theory, does not have any particular bearing on the qualitative nature of the results.

INFLUENCE OF AIR BUBBLES

The presence of air in water has a significant effect only when in the form of bubbles. Dissolved air changes the sound velocity by less than 10 parts per million[33] and the attenuation coefficient at ultra-high frequencies is virtually unchanged within the tolerance of measurement error.[20]

The anomalous attenuation and change in propagation speed for frothy liquids was noted in 1911 by Mallock.[34] A recent survey of the subject is given by Devin.[35] He considers the damping caused by a single bubble in water.

---

*Ref. 15, p. 373

**Ref. 4, p. 762-766, 775-783

Bubbles should have the greatest effect when the sound frequency matches the resonant frequency of the bubble. The resonant frequency of a spherical bubble is given by

$$f_o D = 652$$

where D is the bubble diameter in cm and f_o is the resonance frequency in cycles per second. A bubble resonating at 5.2 kc/s accordingly has a diameter of 1.25 mm and is therefore easily visible. This is pertinent to the interpretation of the measurements discussed in the later chapters.

The conditions under which air bubbles may exist in the ocean are discussed in a number of references.[36-38]

III. DESIGN CONSIDERATIONS

Several materials and cavity shapes were investigated before arriving at the final design. Both cylindrical and spherical chambers were investigated, as well as rectangular prism forms of various relative dimensions. Some of the more important characteristics of the types of chamber which were considered, and reasons for selecting the rectangular or box-shape form in the final design, are discussed in the following sections.

CYLINDRICAL AND SPHERICAL CAVITIES

In the cylindrical cavities the walls were too rigid because of the circular cross section. Hence the bubbles which inevitably formed on the inner wall had a very marked influence on the measurements. The wall could have been made more compliant by introducing corrugations, but this would make it difficult to clean. Moreover, it was found that the seam, produced when a cylinder was fashioned out of a sheet, would disturb the symmetry of the container so much that a poor resonant cavity resulted. Values of Q of the order of 2000 could be obtained from this type of cavity if seamless containers were used, and if proper care were shown. The term Q referred to above represents the quality factor of the cavity response as defined by

$$Q = \frac{f_o}{\Delta f}$$

where f_o is the resonance frequency for a given mode of oscillation and Δf is the bandwidth of the response spectrum for uniform power input as measured at the 3 db level below the resonant peak level. The Q value is inversely proportional to the attenuation coefficient for the cavity or in other words, directly proportional to the

reverberation time. The quality factor characterizes the cavity plus the contained liquid. The above value refers to the cavity filled with nominally pure water. However, it should be noted that any contained bubbles on the walls will tend to produce a low estimate of the Q which would apply for completely degassed water.

A cylindrical cavity in the form of a shallow pan was also investigated. This has the advantage that the free surface and bottom represent the major fraction of the boundary, thus minimizing the area of rigid surface. Good Q factors were obtained, since bubbles do not tend to stick to the bottom and have little effect at the free surface. Bubbles which cling to the cylindrical surface are so far removed from the center that their effect is negligible, since the main reflections take place between top and bottom of the cavity. The main difficulty was that the slightest vibration caused surface waves to be set up. This created difficulties in tuning the cavity, as well as irregularities in the way the sound died out, when the generator was disconnected.

The spherical cavities were obtained by cutting off the neck of commercially available, round-bottom boiling flasks made of Pyrex. Higher Q's can be obtained with these bottles than by any other readily available method, but they suffered from the same limitations as the cylindrical containers to an even more marked degree. The opening in the flasks is so small that cleaning the inside surface is virtually impossible. This type of resonator has been used extensively for research on pure liquids and gases, but was considered unsuited for measurements on sea water with the naturally occurring particulate matter suspended in it. The cylindrical resonators were likewise given up for the same reasons.

BOX-SHAPE CAVITIES

Cavity Properties and Construction

The rectangular prism resonators with free surface have several advantages relative to other forms mentioned:

1. The boundary surfaces are made of flat sheets, and therefore are relatively easy to wipe clean.

2. The boundary will allow pressure release by bending in contrast to the spherical and cylindrical cavities, where pressure release must be accomplished by stretching of the boundary.

3. The sound field in the corners of the box is very weak and theoretically zero in the corner itself. The corners are therefore well suited for support of the cavity.

4. The seams where the sheets are united will naturally fall in the corners, where the effect from them will be at a minimum.

5. The corners allow loose coupling of the transducers, and the coupling can easily be changed.

6. Finally, this type of cavity is relatively easy to manufacture.

The square-cornered cavities therefore seemed to offer the greatest promise and the largest amount of work was devoted to their development.

Cavities were made of a great variety of materials, and in many different sizes. The materials ranged from plastic films and thin shim stock of copper, brass, bronze, and stainless steel, to heavier sheets as well as readily available plastic containers. It was found that stainless steel was superior to any of the other materials. The power loss within the steel sheets is small and the steel alloy is chemically inactive when exposed to sea water. However, stainless steel is not easy to weld or solder.

The original stainless steel cavities had the corners spot-welded to angles made of the same material as the sides. Watertightness was then insured by soft soldering the corners (fig. 1). The supports consisted of four SOAB* rubber blocks, placed as close to the corners as the stability of the cavity would allow. The transducers were immersed in the water as close to the corners as the hum and noise level permitted.

Several attempts were made to improve the construction of the corners of the cavities. It was assumed that the spot-welded and soldered joint would increase the losses of the cavity. Also, the soft-soldered corner had a tendency to leak in time due to electrolytic action, when the cavities were filled with sea water. No really satisfactory solution was found until the NEL machine shop succeeded in developing a technique whereby the corners were inert arc welded. It was not possible to weld sheets thinner than 24 mils, and the final cavities were therefore made of this thickness (fig. 2).

The presence of a few bubbles on the wall did not affect the measurements. A bubble with a resonance frequency close to the measuring frequency of the cavity, however, did have a marked effect. As noted in the introduction, a bubble resonating at 5 kc/s is somewhat larger than 1 mm in diameter and can be detected quite readily and removed. The above frequency corresponds roughly to that of the fundamental mode for the cavity dimensions employed in the sea water measurements reported in section V. A large number of evenly distributed small bubbles will be produced on the walls if air-saturated water is allowed to heat up in a cavity without disturbance, and they will have a marked influence on the measurements. This problem is discussed further in section V.

---

*Previously made by B. F. Goodrich Rubber Co., Akron, Ohio.

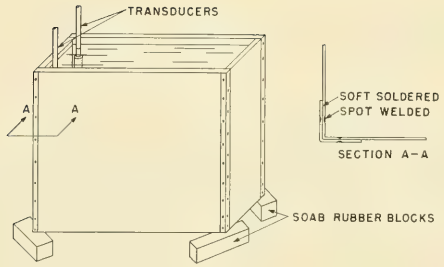

Figure 1. Schematic of preliminary watertight cavity.

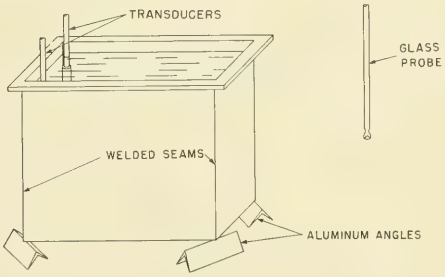

Figure 2. Schematic of final cavity design.

Five different box cavities with welded corners were constructed. The dimensions (all in inches) are as follows:

	Length	Width	Depth
No. 1	17	11	14
No. 2	12	8	10
No. 3	$8\frac{1}{2}$	$5\frac{1}{2}$	7
No. 4	6	4	5
No. 5	$4\frac{1}{4}$	$2\frac{1}{4}$	$3\frac{1}{2}$

Cavity No. 2 was used almost exclusively during the data collection.

Cavity Supports

The rubber supports shown in figure 1 were not very satisfactory. The cavities had to rest on a large area of the support in order to assure stability. Wire supports were attempted and these resulted in the improvement of the Q factor but made cleaning of the side-walls quite difficult. A further difficulty was that the whole cavity would oscillate like a pendulum at a low frequency, and thereby set up wave motion on the rather large free water surface.

The supports finally adopted, and used throughout the data collection, did not have any of these shortcomings. They consisted of four pieces of angle aluminum. The line of support was approximately $\frac{1}{8}$ inch from the extreme corner of the cavity (fig. 2). No increase in the total cavity loss occurred if the supports were moved away from the corners by as much as an additional $\frac{1}{8}$ inch. This was regarded as evidence that the loss due to this type of support was insignificant. In any event, the residual loss caused by the supports if present is taken into account in the calibration of the cavity with distilled water. The aluminum angle supports were used throughout the data collection phase of the work reported here.

Power Supply to Cavity

Different methods of driving the cavities were tried in order to minimize the losses due to the transducers, and at the same time obtain as convenient an instrument as possible. Provision of power input direct to the cavity wall was attempted by gluing a ring of radially polarized barium titanate to it and touching the side with a point driven by a specially constructed electromagnetic system. However, the cavity Q was degraded seriously by this procedure. The simplest driving methods proved to be the best. Two small transducers made from barium titanate cylinders were immersed in the water close to

two corners (fig. 1 and 2). The amount of coupling could then be controlled by moving the transducers closer to or further away from the corners.

The transducers first utilized (shown in cross section in fig. 3B) were found superior in performance to the usual type (fig. 3A). However, the losses introduced by the transducers were still significant, since it was possible to improve the over-all Q of the resonant cavity by moving the transducers closer to the corners. An effort was therefore made to improve the transducers.

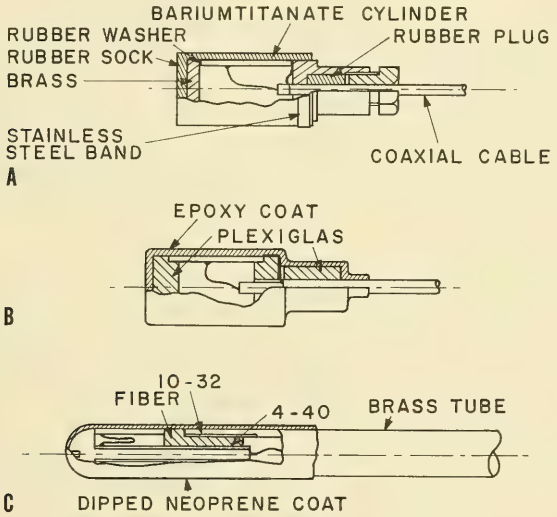

Figure 3. Sound transducers. A, B, preliminary models; C, final design.

The final transducer design is shown in figure 3C. The greatest improvements were accomplished by omitting all soft material between the cylinder and the metal parts, and by using an exterior coating of dipped Neoprene rubber. The soft gaskets used in the transducer (fig. 3A) were replaced by a very thin film of epoxy cement, and it may be

supposed that the cylinder is virtually clamped to the metal end pieces. All motion therefore takes place in the barium titanate cylinder, and this ceramic material has a much smaller mechanical loss than that associated with motion in the rubber gaskets. This improvement is achieved at the cost of a lower sensitivity of the transducer, but experiments indicated that this loss was offset by the fact that the transducers could be coupled closer without affecting the cavity performance.

The Neoprene-rubber solution used for dipping the transducers is made so thin that bubbles are easily seen and can be eliminated before the rubber sets. Also, it is possible to prevent bubbles from forming if care is exercised during the dipping process. Four or five coats are apparently sufficient, since the transducers have been in use for almost a year without any significant deterioration. The loss introduced by the transducers can be neglected for all conditions except where the total losses are an absolute minimum.

The block diagrams in figure 4A and 4B show two possible measuring arrangements that were investigated. Figure 4A is a "sing-around" circuit, where a signal present in the cavity will be picked up by the receiving hydrophone, amplified, and reintroduced in the cavity. The sing-around frequency will be a natural resonance frequency of the cavity, if the electronic circuitry is properly adjusted. The transmission loss from the input terminals of the transmitting hydrophone to the output terminals of the receiving hydrophone is approximately 80 db. The amplifier must therefore supply at least 80-db amplification to establish a sing-around condition, and experience has demonstrated that it is extremely difficult to keep the system functioning properly under field conditions. The equipment would frequently sing-around on some spurious resonance frequency, and very critical adjustments of the tuned circuit and transducer positions would be required before the measurement could be obtained.

Figure 4B shows a much simpler solution. The generator drives the transmitting cylinder, and the received

signal is measured by a vacuum tube voltmeter. The cavity must now be tuned to resonance manually. However, it is possible to "probe" the cavity with a small captured bubble and ascertain when the desired mode is obtained, by determining the position of the nodal lines with the bubble. This procedure would almost invariably stop the sing-around circuit in figure 4A from oscillating. The frequency can be changed in small increments by the cycles increment dial on the generator and the Q factor can be evaluated in this fashion, when the losses are large.

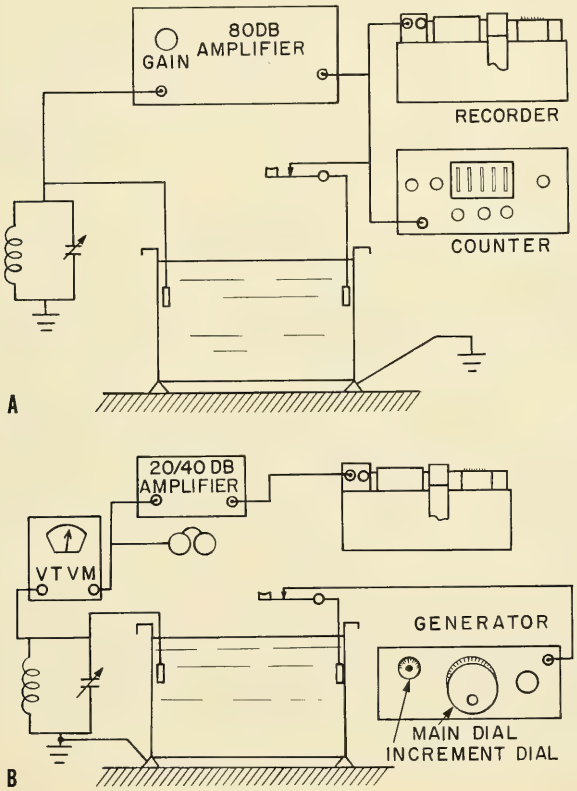

Figure 4. Diagrams of measuring systems. A, preliminary system; B, system employed in final tests.

The best method for lower losses was to record the reverberation process with a Brüel and Kjaer recorder. Examples of records obtained in this manner are given in figures 5 to 7. The permanent record obtained can be studied in detail later on. Small undulations of the free water surface during the measurements will not be too detrimental, since only the envelope of the signal is measured and the frequency at any moment is immaterial. The relationship between the bandwidth Δf in c/s and the reverberation time t in seconds is expressed by $t\Delta f = 2.2$. This relationship was deduced by assuming that the response curve for the cavity is the same as that of a simple electric resonant circuit. This relationship was checked in many instances, where both t and Δf could be obtained independently and no significant discrepancy was ever observed. The reverberation time, however, has been used exclusively for the data-taking phase.

A few comments are appropriate in respect to the hum and noise problem. The input voltage to the transmitting hydrophone was approximately 50v. The output voltage measured by the VTVM (fig. 4B) was approximately 5mv as a maximum value, and voltage levels 50 db below this value were measured when the reverberation curve was recorded. Careful shielding and grounding techniques were essential. The tuned resonant circuit shown in figure 4B was necessary to overcome the remaining hum and structural noise as far as possible and to increase the signal sufficiently for the measurements to take place.

The Q of the electrical tuning circuit in figure 4B was measured independently. It was 60 to 80, depending on the frequency used. This corresponds to a reverberation time of about 1/10 of the shortest reverberation that the equipment could record, and was considered insignificant.

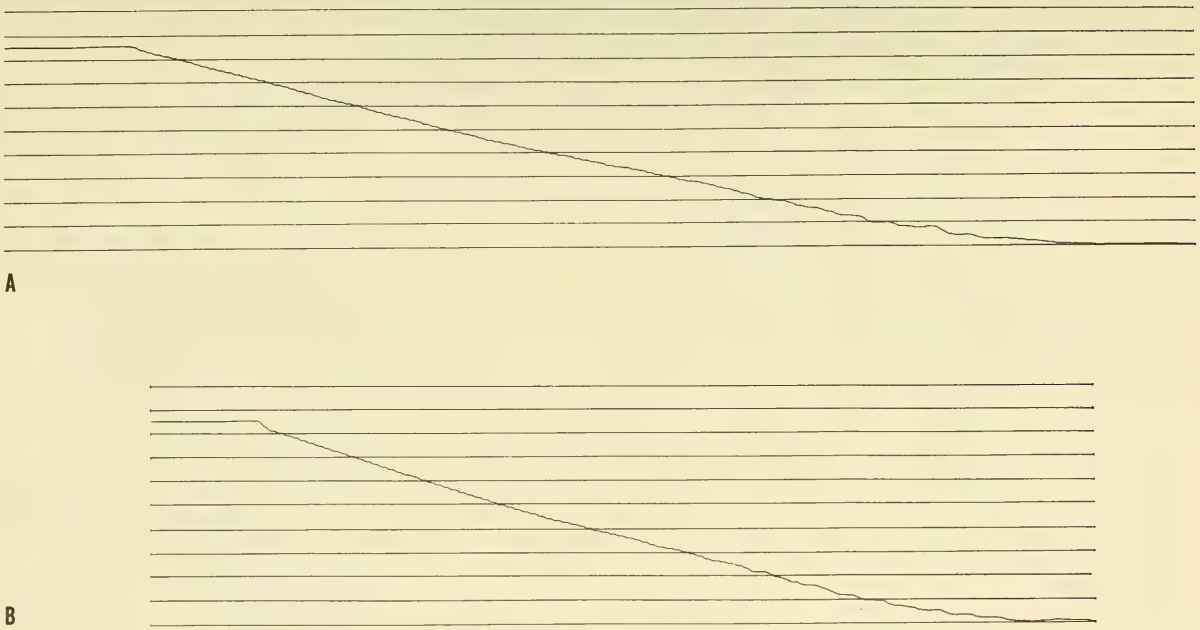

Figure 5. Effects of captured bubble on reverberation time.

A. Typical reverberation curve obtained from calibration tests for mode 1-1-1 using pure water at 19.1°C; resonance frequency, f_o, 5126 c/s; reverberation time, t, 2.81 sec; attenuation, α_o, 12.6 db/kyd.

B. Influence on reverberation time due to presence of an air bubble of 2.5-mm diameter (other conditions nominally the same as for fig. A). Bubble resonance frequency, f, $\approx$ 2600 c/s; t, 2.29 sec; α_{tot}, 15.96 db/kyd.

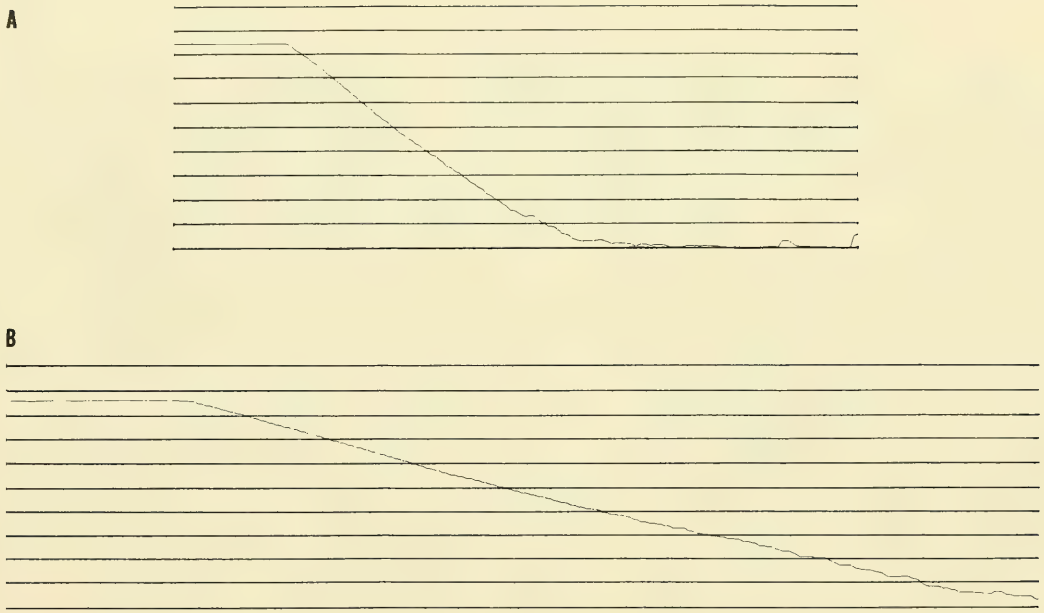

Figure 6. Effects of captured bubble on reverberation time.
A. Influence on reverberation time due to presence of bubble of 1-mm diameter; t, 0.90 sec; α_{tot}, 40.6 db/kyd; f_o, 5154 c/s; f, 6500 c/s. (Other conditions nominally the same as for fig. 5A.)
B. Rerun of conditions of figure 5A without bubble.

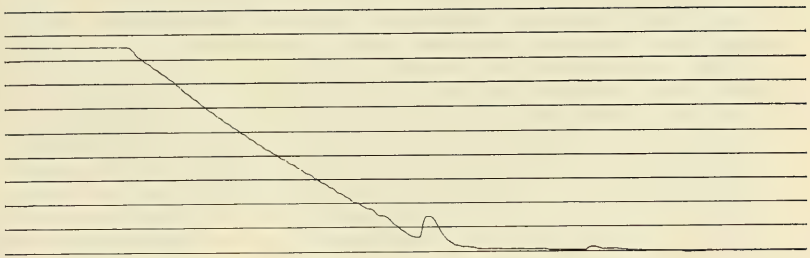

Figure 7. Influence on reverberation time due to presence of bubble of 0.2-mm diameter; f_o, 5139 c/s; T, 19.1°C; $f \approx 32,000$ c/s; t, 1.04 sec; α_{tot}, 35.0 db/kyd. (Other conditions nominally the same as for fig. 5A.)

Figure 8 is a photograph of the equipment used during the data collection in the summer of 1960.

Figure 8. Data-collecting equipment.

IV. THEORETICAL DISCUSSION

The theory of an acoustically resonant chamber is examined here, to develop pertinent relations for the natural frequencies and the particular attenuation factors which are related to the chamber geometry and the contained fluid. For a chamber which contains an ideal, inviscid pure fluid, free of any trapped gas phase, the primary loss of acoustic energy occurs at the walls and free surface by radiation to the environment. The amount of such loss depends upon the configuration of the chamber, the flexural properties of the walls, and the acoustic impedance of the environment compared with that of the fluid.

For a chamber containing a complex fluid mixture like sea water, the additional attenuation which occurs is closely related to the irreversible processes associated with viscosity, heat conduction, and diffusion. In the present analysis only the viscous loss is considered. However, from a phenomenological point of view, all internal losses can be expressed in terms of an equivalent viscosity effect. For sea water the effective viscosity can be several orders of magnitude greater than the actual viscosity.

The notation in the ensuing discussion is patterned after that of A. Sommerfield.[39] The development starts with the formulation of the wave equation for acoustical disturbances in a viscous fluid. Vortex motion and gravity wave modes are excluded at the outset by adopting the conventional approximations of acoustic theory.

ACOUSTICAL WAVE EQUATION FOR VISCOUS FLUIDS

Fundamental Equations*

The Navier-Stokes form of the equation of motion for a viscous fluid is

$$\rho \frac{\partial \hat{v}}{\partial t} + \rho (\hat{v} \cdot \nabla) \hat{v} - \mu_1 \nabla^2 \hat{v} - (\mu_1 + \lambda_1) \nabla (\nabla \cdot \hat{v}) + \nabla P = \rho \hat{F} \qquad (1)$$

where ρ is fluid density, $\hat{v}$ is the velocity vector, P the pressure, $\hat{F}$ the body force per unit mass, μ_1 and λ_1 the first and second viscosity coefficients and ∇ is the general (three-dimensional) gradient operator. The velocity and density must also satisfy the continuity equation

$$\frac{\partial \rho}{\partial t} + \nabla \cdot (\rho \hat{v}) = 0 \qquad (2)$$

In addition it is presumed that ρ and P are related by an equation of state, which can be expressed in a purely formal way as

$$P = f(\rho) \qquad (3)$$

Relation (3) in effect ignores any temperature dependence; however, this is unimportant for liquids since the temperature variation can be considered virtually nil. This matter is explored in more detail in pages 37-38.

---

*A list of symbols is given on page iv.

Assumptions

The additional stipulations regarding the nature of the disturbances are the following:

(a) The changes in P, $\hat{v}$, and ρ associated with the acoustic disturbance are regarded as sufficiently small that the usual linearizing approximation can be made. Specifically, the anomalies of p and ρ are regarded as small compared to their respective mean values within the chamber. Also $\hat{v}$ is regarded as small compared with the speed of sound for the fluid occupying the chamber.

(b) The motion is regarded as irrotational,

$$\nabla \times \hat{v} = 0$$

(c) It is presumed that there is no net translation of the medium.

(d) The body forces (including gravity) are considered to have negligible influence on the acoustic disturbances.

Linearized Relations

In view of conditions (a), (c), and (d), relations (1) and (2) can be approximated by

$$\rho_o \frac{\partial \hat{v}}{\partial t} - \mu_1 \nabla^2 \hat{v} - (\mu_1 + \lambda_1) \nabla (\nabla \cdot \hat{v}) + \nabla p = 0 \qquad (1a)$$

$$\frac{\partial \rho}{\partial t} + \rho_o \nabla \cdot \hat{v} = 0 \qquad (2a)$$

where ρ_o is the mean density and p is the departure of the pressure from hydrostatic.

Following usual acoustical procedure, a mixed Lagrangian-Eulerian system is employed in which the particle displacement vector $\hat{s}$ is regarded as a field variable. Specifically $\hat{r} + \hat{s}$ represents the position vector at time t of that particle whose equilibrium position is $\hat{r}$. In view of the condition of small displacement implied by condition (a) it follows that

$$\frac{\partial \hat{s}}{\partial t} = \hat{v} \tag{4}$$

Accordingly (2a) can be expressed as

$$\frac{\partial}{\partial t} (\rho + \rho_o \nabla \cdot \hat{s}) = 0$$

or

$$(\rho - \rho_o) = -\rho_o \nabla \cdot \hat{s} = -\rho_o \Theta \tag{5}$$

where Θ is a convenient notation for the dilation $\nabla \cdot \hat{s}$.

Equation (3) implies that for small changes

$$\Delta P = \frac{dP}{d\rho} \Delta \rho = \lambda_o \frac{\Delta \rho}{\rho_o} \tag{6}$$

where λ_o is the second Lame parameter (or reciprocal compressibility). Using (5) and taking ΔP as the acoustic pressure anomaly (p) yields

$$p = -\lambda_o \Theta \tag{7}$$

which is an adequate approximation for acoustic waves whose intensity is not excessive.

The Stress Tensor

In the absence of viscosity the acoustic stress tensor* in a fluid is given by

$$\tau_{ik} = \lambda_o \Theta \delta_{ik} \tag{8}$$

where δ_{ik} is the unit tensor (which has unit value for $i = k$ and vanishes for $i \neq k$). Relation (8) is a compact statement for the isotropy of the normal stress in an inviscid fluid.

For an elastic solid which is in a state of strain relative to an equilibrium state, the associated elastic stress is given by the non-isotropic tensor

$$\tau_{ik} = \mu_o D_{ik} + \lambda_o \Theta \delta_{ik} \tag{9}$$

Here D_{ik} is the strain (or deformation) tensor

$$D_{ik} = \frac{\delta s_i}{\delta x_k} + \frac{\delta s_k}{\delta x_i} \tag{10}$$

where s_i is the components of the vector displacement $\hat{s}$ relative to the relaxed(equilibrium) state and μ_o is the first Lame parameter. The elastic tensor is symmetric in the sense that $\tau_{ik} = \tau_{ki}$, which implies that there are basically three different shear stress terms and three different normal stress terms. Relation (9) would be

---

*The stress tensor τ_{ik} as employed here is such that tensile stresses τ_{11}, τ_{22}, τ_{33} are positive or pressures negative. The conventional indicial notation is employed, where i, k can take on values 1, 2, 3 independently.

pertinent to the cavity walls, assuming that the latter could be considered elastic.

For a visco-elastic medium, relation (9) should be supplemented by the viscous stresses which depend upon the rate of deformation and rate of dilatation of the medium. The complete stress tensor in this case is

$$\tau_{ik} = \mu_o D_{ik} + \lambda_o \Theta \delta_{ik} + \mu_1 \frac{\partial D_{ik}}{\partial t} + \lambda_1 \frac{\partial \Theta}{\partial t} \delta_{ik} \qquad (11)$$

which retains the symmetry property mentioned earlier. The Navier-Stokes equation for a viscous fluid as given by (1) employs (11) with $\mu_o = 0$ and $-\lambda_o \Theta$ replaced by the fluid pressure P.

As required by the second law of thermodynamics, the viscous stresses can never lead to a decrease of the entropy in a closed system. Eckart* has shown that this will be assured under all conditions of deformation, if and only if

$$\mu_1 \geq 0 \text{ and } \lambda_1 \geq -\tfrac{2}{3} \mu_1 \qquad (12)$$

It may be remarked that the traditional stipulation regarding the second viscosity coefficient (namely $\lambda_1 = -\frac{2}{3}\mu_1$) just barely satisfies condition (12). This is important from the standpoint of loss of acoustic energy associated with the irreversible processes within the system. The rate of conversion of the dynamic (acoustic) energy to thermal energy is directly related to the rate of increase of the entropy due to internal processes. Clearly the latter is enhanced if λ_1 exceeds the lower limit imposed by (12).

---

*Carl Eckart, unpublished class notes on Principles of Hydrodynamics, Scripps Institution, University of California, 1948.

The Acoustic Wave Equation

In view of the identity

$$\nabla (\nabla \cdot \hat{v}) = \nabla^2 \hat{v} + \nabla \times (\nabla \times \hat{v}) \tag{13}$$

it follows that for irrotational motion (condition b), the equation of motion (1a) simplifies to

$$\rho_o \frac{\partial \hat{v}}{\partial t} - (2\mu_1 + \lambda_1) \nabla^2 \hat{v} + \nabla p = 0 \tag{14}$$

Moreover, if (4) and (7) are employed then the latter relation is rendered in the form of a wave equation for the displacement $\hat{s}$:

$$\rho_o \frac{\partial^2 \hat{s}}{\partial t^2} = \lambda_o \nabla^2 \hat{s} + (2\mu_1 + \lambda_1) \nabla^2 \frac{\partial \hat{s}}{\partial t} \tag{15}$$

The basic form of the wave equation remains unchanged for a visco-elastic medium; the only modification is the replacement of λ_o by $2\mu_o + \lambda_o$. However, the boundary conditions appropriate to the visco-elastic problem are certainly more elaborate than those required in the viscous fluid problem.

In the special case of an inviscid fluid, (15) reduces immediately to the canonical form for simple waves

$$\frac{\partial^2 \hat{s}}{\partial t^2} = c^2 \nabla^2 \hat{s} \tag{15a}$$

where $c = \sqrt{\lambda_o / \rho_o}$ represents the wave speed.

Relation (15) holds equally well for $\hat{v}$, Θ, or p. The choice of dependent variable depends largely on the nature of the boundary conditions. In any event, $\hat{v}$, Θ, and p are readily determined in terms of $\hat{s}$.

Boundary Conditions

The dynamic and kinematic boundary conditions require that continuity exist in respect to the displacement and stresses at the boundaries of the system. Specifically, if Δ denotes the difference in a given quantity across the boundary of the system then it is required that

$$\begin{aligned} \Delta\hat{s} &= 0 \\ \Delta(n_k \tau_{ik}) &= 0 \end{aligned} \tag{16}$$

where n_k denotes the direction cosines of the normal to boundary surface.

If the boundary is a liquid-air interface, and if both fluids are considered inviscid, then it is sufficient to stipulate only

$$\begin{aligned} \Delta s_n &= 0 \\ \Delta p &= 0 \end{aligned} \tag{17}$$

If the air is neglected altogether, then the second condition is sufficient and implies simply that $p = 0$ on a truly free surface.

In the case of a thin flexible sheet separating two inviscid fluids, where the sheet can support significant tensile stress, then the stress condition of (16) can be replaced by

the condition that the change of p across the sheet is proportional to the curvature and tension in the sheet. However, the latter in turn is dependent upon the distortion of the sheet, which requires the solution of a separate elastic problem for the sheet, with its attendant end conditions regarding rigidity.

Associated Energy Equation

In many cases one can bypass some of the mathematical complexities involved in the detailed analysis of the dynamic problem by considering the energy budget alone, or at least as a supplementary relation. The real utility of the energy relation is associated with its inherent appeal from the standpoint of physical understanding of the problem.

In order to form the energy relation associated with the acoustic wave phenomena, relations (2a), (6), and (14) are convenient as a starting point. Using the definition of λ_o stipulated by (6), the continuity relation is readily rendered in the form

$$\frac{1}{\lambda_o} \frac{\partial p}{\partial t} + \nabla \cdot \hat{v} = 0 \tag{18}$$

By forming the scalar product of $\hat{v}$ on relation (14), multiplying (18) by p, and then adding the two resulting equations, the following quadratic relation is obtained

$$\frac{\partial}{\partial t} \left\{ \tfrac{1}{2} \rho_o v^2 + \frac{p^2}{2\lambda_o} \right\} + \nabla \cdot (p\hat{v}) = (2\mu_1 + \lambda_1)\, \hat{v} \cdot \nabla^2 \hat{v} \tag{19}$$

where v is the magnitude of the particle velocity. This is the energy relation associated with acoustic disturbances (of sufficiently small energy) in a viscous fluid.

The terms $\rho_o v^2/2$ and $p^2/2\lambda_o$ represent, respectively,

the kinetic energy and intrinsic energy of the dilatational oscillations, both expressed as energy density (energy per unit volume). The intrinsic energy is really a measure of the departure of the internal energy from that at equilibrium due to compression or dilatation of the fluid.

The term $p\hat{v}$ represents the energy flux or transmission of energy per unit time through a unit area. For a transducer which radiates acoustic energy outwards in a fluid medium, the acoustic power of the transducer is given by the integral

$$\int\int_S \overline{p\hat{v}} \cdot d\hat{\sigma}$$

which is evaluated over the exterior surface of the transducer, the surface element $d\hat{\sigma}$ being associated (in direction) with the outward normal to the surface of the transducer.

The viscous term on the right side of (19) can be rewritten in several different forms depending upon the nature of the flow. Under the approximation of irrotational flow as employed in (14) and in view of (18), it can be shown that the viscous term of the energy equation can be expressed as

$$\frac{(2\mu_1 + \lambda_1)}{\lambda_o} \left\{ \nabla \cdot \left[\hat{v} \frac{\partial p}{\partial t} \right] + \frac{1}{\lambda_o} \left[\frac{\partial p}{\partial t} \right]^2 \right\}$$

Substituting the latter expression in (19) yields the following energy equation appropriate to conditions of irrotational acoustic disturbances in a viscous fluid:

$$\frac{\partial}{\partial t} \left\{ \frac{\rho_o v^2}{2} + \frac{p^2}{2\lambda_o} \right\} + \nabla \cdot \left\{ \hat{v} \left[p + \beta \frac{\partial p}{\partial t} \right] \right\} = -\frac{\beta}{\lambda_o} \left[\frac{\partial p}{\partial t} \right]^2 \qquad (20)$$

where

$$\beta = \frac{2\mu_1 + \lambda_1}{\lambda_o} \tag{21}$$

The latter parameter has the dimensions of time and can be regarded as a characteristic relaxation time associated with the damping action of viscosity on acoustic oscillations.

In order to appreciate the full significance of relation (20), it is instructive to consider the integral of this relation for a finite fluid volume V bounded by the closed surface S. By employing the divergence theorem, the integral relation takes the form

$$\frac{\partial E}{\partial t} = -\int\int\int_V \frac{\beta}{\lambda_o}\left(\frac{\partial p}{\partial t}\right)^2 dV - \int\int_S v_n\left(p + \beta\frac{\partial p}{\partial t}\right) d\sigma \tag{22}$$

where E is the total acoustic energy in the volume V. If the surface S is not simply connected, then one can regard the surface integral as a sum of integrals over the pertinent exterior and interior surfaces. The normal component of velocity v_n in every case is taken positive if the flow is towards the surface from the fluid volume concerned.

For an inviscid fluid, (22) reduces immediately to

$$\frac{\partial E}{\partial t} = -\int\int_S v_n\, p\, d\sigma \tag{22a}$$

which stipulates simply that the change in acoustic energy in the volume V equals the net rate of influx of energy across the closed surface S which delineates this volume. For free vibrations, the acoustic energy level can be maintained only if there is total reflection of energy at

the bounding surface. This requires that $v_n = 0$ or that $p = 0$ on the surface, a situation which is approached only if a large difference in acoustic impedance (ρc) exists across the bounding surface.

In the case of the viscous fluid, even if p or v_n vanishes on the bounding surface of the medium, the energy of free acoustic vibrations will decay at a rate depending upon the square of the time rate of change of p. If the disturbances are nearly simple harmonic (except for a slow decay) then

$$\overline{\frac{\partial p^2}{\partial t}} \cong \omega^2 \overline{p^2}$$

where ω is the frequency (radians/second) and the bar indicates a time average over an integral number of oscillations. Moreover, the energy E can be considered (on the average) as half kinetic and half intrinsic. Accordingly, it follows from (22) that, for total reflection at the bounding surface S,

$$\frac{\partial \overline{E}}{\partial t} = -\beta\omega^2 \overline{E} \tag{22b}$$

or

$$\overline{E} = E_o e^{-\beta\omega^2 t} \tag{23}$$

If energy does radiate through the bounding surface at a rate proportional to the mean energy density (E/V) within the medium then the damping modulus $\beta\omega^2$ in (23) must be replaced by

$$\left(\beta\omega^2 + \gamma_t \frac{cA}{V}\right)$$

where c is the wave speed, A the surface area, V the volume and γ_t a transmission coefficient dependent upon the impedance mismatch between the medium and its environment. For small volumes, the second term (radiational loss) will dominate, while for sufficiently large volumes the viscous term will ultimately dominate.

The above deductions, which have been obtained in a somewhat heuristic manner, will be derived more rigorously in the development which follows.

Effect of Temperature Fluctuations*

The question of temperature fluctuations associated with acoustic disturbances was avoided at the outset by adopting relation (3). Actually the equation of state for any pure substance should involve a third thermodynamic variable, the absolute temperature T being a possible choice.

Thus formally one should stipulate that for the particular medium

$$\rho = f(P, T) \tag{24}$$

The differential counterpart of this is

$$\frac{1}{\rho} d\rho = K\, dP - b\, dT \tag{25}$$

where K is the isothermal compressibility and b the(volumetric) coefficient of thermal expansion. Relation (3) and its differential counterpart (6) can be consistent with

---

*The following section as well as that on energy considerations was suggested by R. O. Reid.

(24) only if the change in T is proportional to that of P or that the temperature is constant. The second condition would require that λ_o^{-1} be identified with the isothermal compressibility, a deduction which is known a posteriori to be incorrect for acoustic waves in gases.* The other possibility requires that

$$dP = \frac{\lambda_o}{\rho} d\rho = A\, dT \tag{26}$$

where A is an appropriate coefficient. The three parametric relations implied by (26) represent the differential equations for a curve in the ρ, P, T diagram. Clearly this curve must lie on the equation of state "surface" given by (24). Except for this constraint, the curve is arbitrary.

In order to remove the ambiguity regarding the thermodynamic path, it is evident that a further relation between the thermodynamic variables is needed. Such a relation could be provided a priori by stipulating that the path is adiabatic. This requires a definite relation between P and T which is given by Kelvin's equation

$$dT = \frac{bT}{\rho C_p} dP \tag{27}$$

where C_p is the specific heat at constant pressure. This implies in turn that A^{-1} is the coefficient in (27) and that

$$\lambda_o^{-1} = K - \frac{b^2 T}{\rho C_p} \tag{28}$$

---

*This would lead to the Newtonian expression for the speed of sound, which is known to be less than the measured values.

which represents the adiabatic compressibility. For liquids, the value of K is much greater than the second term in (28) and hence it makes little difference, in respect to the sound speed, whether one uses the adiabatic or isothermal compressibility (except in problems involving refraction of sound rays).

The physical justification of the assumption of adiabatic changes of state lies largely in the notion that acoustically induced heat conduction, like viscous generation of heat, will be of second order compared with the change in intrinsic energy which occurs in an acoustic vibration. When one neglects both viscosity and heat conduction, the resulting acoustic theory predicts reasonably accurate propagational speeds. However, no information is obtained regarding the attenuation which is associated with irreversible processes.

A good approximation of the viscous damping is achieved for acoustic waves by ignoring vorticity, in spite of the fact that viscosity introduces a flux of vorticity inwards from the boundaries, if shearing motion occurs at the boundaries. The approximation is justifiable for acoustic disturbances since the rate of dilatation is much larger than the vorticity. A similar sort of approximation can be made in considering the effect of heat conduction. Although the latter causes a change in entropy of the medium, the process can be considered nearly isentropic.

If there exists a small departure of the specific entropy (ergs/gm °K) from its mean value, then relation (7) should be replaced by

$$p = \frac{bT_o \lambda_o}{C_p} \eta - \lambda_o \Theta \tag{29}$$

where T_o is the mean temperature, η the anomaly of specific entropy and λ_o has the meaning implied by (28). For isentropic conditions this obviously reduces to (7) as a special case. Let the flux of heat be given by $-K \nabla T_1$ where K is

the conductivity and T_1 the anomaly of temperature from the mean value T_o. The linear approximation* for the change in η is accordingly given by

$$\frac{\partial \eta}{\partial t} = \frac{K}{\rho_o T_o} \nabla^2 T_1 \tag{30}$$

Now since the process is considered nearly isentropic, it is reasonable to suppose that (27) can be employed as an approximation for T_1 in terms of p, with T and ρ taken as their mean values and T_1 and p identified with dT and dP respectively. This approximation renders (30) in the form

$$\frac{\partial \eta}{\partial t} = \frac{Kb}{\rho_o^2 C_p} \nabla^2 p \tag{31}$$

Accordingly (29) can be approximated by

$$\frac{\partial p}{\partial t} = \frac{\varkappa b^2 T_o \lambda_o}{\rho_o C_p} \nabla^2 p - \lambda_o \frac{\partial \Theta}{\partial t} \tag{32}$$

where $\varkappa$ is the thermal diffusivity $(K/\rho_o C_p)$. Relation (32) implies that the plot of p versus Θ depends upon the characteristics of the acoustic waves (e.g., the frequency) as well as the properties of the medium. Moreover, p and Θ are not exactly in phase as implied by (7).

If (32) is employed in place of (7) then the wave equation (in terms of p) takes the form

$$\rho_o \frac{\partial^2 p}{\partial t^2} = \lambda_o \nabla^2 \left\{ p + \left(\beta + \frac{\varkappa b^2 T_o}{C_p} \right) \frac{\partial p}{\partial t} \right\} \tag{33}$$

---

*There will exist a steady increase of η with time associated with the attenuation; however, this is of second order.

Thus the attenuation factor β associated with viscosity is supplemented by an additional term related to the thermal conductivity of the medium. For water the magnitude of the attenuation associated with conductivity is about 1/10 of that due to viscosity under normal conditions. In view of this, the neglect of conductivity seems to be justifiable. However, for greater accuracy, the effect of conduction can be included within the framework of the viscous theory alone by employing the quantity

$$\left\{ (2\mu_1 + \lambda_1) + \frac{\varkappa b^2 T_o \lambda_o}{C_p} \right\}$$

as an effective viscosity in place of $(2\mu_1 + \lambda_1)$.

SOME SPECIAL SOLUTIONS OF THE WAVE EQUATION

Plane-Attenuated Sound Wave

The particle displacement for a simple harmonic, plane sound wave, in a fluid with viscous losses and progressing in the x-direction, can be written

$$\varepsilon = \varepsilon_o e^{j(\omega t - kx)} e^{-\alpha_k x} \tag{34}$$

where $j = \sqrt{-1}$, k is the wave number, ω the frequency and ε_o is the amplitude of excursion of the fluid particles. The last term containing α_k is the attenuation term. This can be included in the propagation constant by allowing k to assume complex values. The complex wave number k^* is accordingly

$$k^* = k - j\,\alpha_k \tag{34}$$

Hence, (33) takes the form

$$s = s_o e^{j(\omega t - k^* x)} \tag{35}$$

For simple harmonic waves it follows that

$$\frac{\partial s}{\partial t} = j\omega s \tag{36}$$

and therefore the scalar counterpart of (15) takes the form

$$\frac{\partial^2 s}{\partial t^2} = \frac{\lambda_o}{\rho_o}(1+j\omega\beta)\frac{\partial^2 s}{\partial x^2} \tag{37}$$

where β is the viscous time factor defined by (21). It is convenient to introduce a complex sound speed

$$c^* = \left(\frac{\lambda_o}{\rho_o}\right)^{\frac{1}{2}}(1+j\omega\beta)^{\frac{1}{2}} \tag{38}$$

and thereby recover the canonical form

$$\frac{\partial^2 s}{\partial t^2} = c^{*2}\frac{\partial^2 s}{\partial x^2} \tag{39}$$

The relation (35) is consistent with (39) provided that

$$c^* k^* = \omega \tag{40}$$

where ω is regarded as real. Thus the complex wave number is given by

$$k - j\alpha_k = \omega\left(\frac{\lambda_o}{\rho_o}\right)^{-\frac{1}{2}}(1+j\omega\beta)^{-\frac{1}{2}} \tag{41}$$

Expansion of the term on the right as a power series in $\omega\beta$ and separating real and imaginary parts gives

$$\text{(a)}\quad k = \frac{\omega}{c}\left[1 - \frac{3}{8}(\omega\beta)^2 - \ldots\right]$$

$$\text{(b)}\quad \alpha_k = \frac{\omega^2\beta}{2c}\left[1 - \frac{5}{8}(\omega\beta)^2 - \ldots\right] \tag{42}$$

where c is the wave speed $\sqrt{\lambda_o/\rho_o}$. If $\omega\beta$ is much less than unity, then the above relations can be approximated by

$$k = \frac{\omega}{c} \text{ and } \alpha_k = \frac{\omega^2\beta}{2c} = \frac{k\omega\beta}{2} \tag{43}$$

These approximations apply as long as the viscous components of the stress tensor (11) are small compared with the elastic part. Thus, to this order of approximation there is no influence of viscosity on the wave number-frequency relation, while the spatial attenuation coefficient is directly proportional to the viscosity. The above attenuation factor differs from that given in the energy considerations in two respects. First, the factor c enters since α_k is an attenuation coefficient per unit length along the wave ray. Second, the factor $\frac{1}{2}$ enters since α_k pertains to the amplitude attenuation coefficient rather than the energy attenuation. Bearing this in mind, the result (43) is entirely consistent with the earlier deductions.

If one takes as a lower limit, $\lambda_1 = -2\mu_1/3$, then it is readily shown that

$$\alpha = \frac{2}{3}\frac{\omega^2\mu_1}{\rho_o c^3} \tag{44}$$

which is the result obtained by Stokes. However, for some fluids the numerical factor in (44) may be significantly greater than $\frac{2}{3}$, in view of conditions (12).

Cavity Theory - Inviscid Fluid

The resonators used for the measurements have been discussed in a previous section. For the present development it will suffice to know that they are made of stainless steel sheets in the shape of a square-cornered tank. In the following computations an orthogonal Cartesian coordinate system is employed with the three axes labeled (x_1, x_2, x_3). The tank is taken in the positive octant with a corner in (0, 0, 0). The three coordinate planes will then coincide with three sides of the tank. The corner diagonally opposite (0, 0, 0) is labeled (ℓ_1, ℓ_2, ℓ_3).

The wave equation for loss free fluids is given by (15a). A possible solution of this wave equation is given by

$$S_i = A_i \cosh (K_i x_i + \psi_i) \sinh (K_j x_j + \psi_j) \sinh (K_k x_k + \psi_k) e^{-\Omega t} \quad (45)$$

where the subscripts i, j, k are cyclic. The value of the subscript designates the particular component, in the same sense as the coordinate designation. Each of the quantities A_i, K_i, ψ_i and Ω can take on complex values.

Thus

$$\begin{aligned} K_i &= \alpha_i - jk_i \\ \Omega &= \alpha_t - jw \end{aligned} \quad (46)$$

etc. The wave equation is satisfied provided that

$$\Omega^2 = c^2 \sum_1^3 K_i^2 \quad (47)$$

In regard to boundary conditions, two simple cases will be considered first. These correspond to total reflection of energy at the boundaries of the tank. A more general boundary condition is considered later.

Rectangular Cavity with Hard Walls

If all of the walls are considered absolutely rigid, as a limiting case, then (with $i = 1, 2, 3$)

$$S_i = 0 \text{ at } x_i = 0, \ell_i \tag{48}$$

where ℓ_1, ℓ_2, ℓ_3 denote the dimensions of the cavity. Relations (45) will satisfy the six boundary conditions stipulated by (48) provided that

$$\cosh \psi_i = 0$$

and (49)

$$\cosh (K_i \ell_i + \psi_i) = 0$$

The possible roots of these relations yield

$$\psi_i = \pm j \left(\frac{\pi}{2} + m_i \pi \right)$$

and (50)

$$K_i \ell_i = \pm j n_i \pi$$

where n_i and m_i can take on any integer value independently. The set $n_i(n_1, n_2, n_3)$ designates the particular mode of oscillation; a fundamental mode of oscillation corresponds to the particular set (1, 1, 1). The second of relations (50) demands that K_i be pure imaginary and hence

$$\alpha_i = 0$$

$$k_i = n_i \frac{\pi}{\ell} \tag{51}$$

Moreover, for an inviscid fluid c is real and hence Ω^2 must be negative so that the temporal attenuation factor α_t is zero and the eigenfrequencies of the system are given by

$$\omega = \pi c \left\{ (n_1/\ell_1)^2 + (n_2/\ell_2)^2 + (n_3/\ell_3)^2 \right\}^{\frac{1}{2}} \tag{52}$$

Rectangular Cavity with Soft Walls

The opposite extreme of the previous case is a cavity for which complete pressure release occurs at the boundaries. The pressure is readily evaluated in terms of the relation

$$p = -\lambda_0 \nabla \cdot s \tag{53}$$

if the displacement components s_1, s_2, s_3 are known. Using (45) the relation for p is

$$p = -\lambda_0 \left(\sum_1^3 A_i K_i \right) \prod_1^3 \sinh (K_i x_i + \psi_i) e^{-\Omega t} \tag{54}$$

Now if $p = 0$ on the six planes $x_i = 0, \ell_i$, then it is required that

$$\sinh \psi_i = 0$$
$$\sinh (\psi_i \ell_i + \psi_i) = 0 \tag{55}$$

for $i = 1, 2, 3$. This in turn yields $\alpha_i = 0$ and

$$k_i = n_i(\pi/\ell_i) \tag{56}$$

where $n_i = 0, 1, 2, \ldots$; at least one of the n_i differs from zero for non-trivial solutions. The relation for the wave numbers and eigenfrequencies are thus formally the same as before.

It is possible, of course, to have a mixed boundary condition for which the displacement vanishes on some of the walls and p vanishes on the others.

So far the amplitude factors A_i have been regarded as arbitrary. However, since the vector displacement must satisfy the basic relation

$$\rho_o \frac{\partial^2 \mathcal{S}}{\partial t^2} + \nabla p = 0 \tag{57}$$

it follows that (45) will be valid only if

$$A_i = BK_i \tag{58}$$

where B is a single arbitrary constant. Accordingly the

relation for p takes the form

$$p = -\rho_o B \Omega^2 \prod_1^3 \sinh (K_i x_i + \psi_i) e^{-\Omega t} \tag{59}$$

where (47) and the identity $c = \sqrt{\lambda_o / \rho_o}$ is employed.

Rectangular Cavity with Partially Yielding Walls

For the more general case, the boundary condition can be expressed in terms of the unit area acoustic impedances of the walls. The boundary impedance Z is expressed by

$$Z = R + j X = \frac{p}{v_n} \tag{60}$$

where v_n is the normal component of velocity into the boundary from the interior of the system. It is understood that the various quantities are evaluated at the boundary concerned. Using the relations for displacement and pressure given by (45) and (59) it follows that at $x_1 = 0$

$$Z_1 (0) = -\rho_o \frac{\Omega}{K_1} \tanh \psi_1$$

or

$$\psi_1 = -\tanh^{-1} \frac{Z_1 (0) K_1}{\rho_o \Omega} \tag{61}$$

On the other hand, application of (60) at the boundary $x_1 = \ell_1$ yields

$$Z'_1 = \rho_o \frac{\Omega}{K_1} \tanh (K_1 \ell_1 + \psi_1) \tag{62}$$

The parameter ψ_1 can be eliminated between the latter two equations by use of the identity

$$\tanh(\alpha+\beta) = \frac{\tanh\alpha + \tanh\beta}{1 + \tanh\alpha \tanh\beta}$$

The resulting relation is

$$\tanh K_1 \ell_1 = \frac{K_1}{\rho_o \Omega} \frac{Z_1 + Z'_1}{\left\{ 1 + \left(\frac{K_1}{\rho_o \Omega} \right)^2 Z_1 Z'_1 \right\}} \tag{63}$$

which represents an implicit relation for K_1 in terms of Ω and the boundary impedances Z_1 and Z'_1. This relation can be augmented by the corresponding two equations for the coordinate directions 2 and 3. These three equations, together with

$$\Omega^2 = c^2 \left(K_1^2 + K_2^2 + K_3^2 \right) \tag{64}$$

allow an evaluation of the K_i and Ω in terms of the boundary impedances.

The real parts of Ω and K_i correspond to the temporal and spatial attenuation coefficients and these are regarded as small compared to the imaginary parts. Consequently the approximations

$$K_i^2 = -k_i^2 + j\, 2\, k_i\, \alpha_i$$

$$\Omega^2 = -\omega^2 + j 2 \omega \alpha_t$$

are quite adequate. Making use of these in (64) leads to the approximate relations

$$\text{(a)} \quad \omega^2 = c^2 \sum_{1}^{3} k_i^2$$

$$\text{(b)} \quad \alpha_t = \frac{c^2}{\omega} \sum_{1}^{3} k_i \alpha_i \tag{65}$$

It will be noted that the temporal decay factor α_t in the present case is related entirely to energy leakage through the walls of the tank. It will be shown that this loss is about tenfold greater than the viscous losses when the cavity is filled with pure, gas-free water. However, it is much less than the attenuation as measured with most of the sea water samples.

It remains to consider the transcendental relations of the type (63). The limiting situations for which $Z \to 0$ and $Z^{-1} \to 0$ both lead to

$$\tanh K_1 \ell_1 = 0$$

which corresponds to the special case of total reflection at the walls and zero attenuation. Actually $Z = 0$ corresponds to the extreme soft wall condition and $Z^{-1} = 0$ to the extreme hard wall discussed in the previous sections.

For the case of compliant walls for which $|Z|$ is small compared with the characteristic impedance of the fluid $\rho_o c$, the quadratic term in Z can be neglected in (63) giving

$$\tanh K_1 \ell_1 = \frac{K_1}{\rho_o \omega} \left(Z_1 + Z'_1 \right) \tag{66}$$

Moreover, since the departure of K_1 from the value $K_1(0)$

for zero boundary impedance is small, the expansion of (66) leads to the approximation

$$(\Delta K_1)_\ell = \frac{K_1(0)}{\rho_0 \Omega(0)} \left(Z_1 + Z'_1 \right)$$

where ΔK_1 is the departure from $K_1(0) = j n_1 \pi \ell_1$. This relation can also be expressed as

$$(\Delta K_1)_\ell = \frac{k_1(0)}{\rho_0 \omega(0)} \left(Z_1 + Z'_1 \right) \tag{67}$$

where $k_1(0)$ and $\omega(0)$ are the zero order estimates of the wave number (for direction 1) and the frequency under the condition of zero boundary impedance (hence no loss).

The unit area acoustic impedances of the boundaries can be estimated by assuming that the walls behave like a flexible rectangular membrane with the edges rigidly clamped. The tank employed in the experimental work reported here employs stainless steel sheets of such dimensions that the free resonance frequencies of the walls are much less than the resonance frequencies corresponding to the cavity modes. The load of the wall can therefore be considered as a combination of a resistive and mass load such that

$$Z = r + j \omega m \tag{68}$$

where r is the loss resistance per unit area and m is the mass per unit area.

Setting $\left(Z_1 + Z'_1 \right) = r_1 + j \omega m$, in relation (67) and separating the real and imaginary parts yields

$$\text{(a)} \quad \alpha_1 = \frac{k_1(0)}{\rho_o \omega(0) \ell_1} r_1$$

$$\text{(b)} \quad \Delta k_1 = \frac{-k_1(0)}{\rho_o \ell_1} m_1 \tag{69}$$

Relation (69a) shows that the spatial attenuation factor α_1 is directly proportional to the resistive factor r_1, the proportionality factor being dependent upon the resonant mode and cavity dimensions. Using $k_1(0) = n_1 \pi / \ell_1$ yields

$$\alpha_1 = \frac{\pi}{\rho_o \omega(0)} \frac{n_1}{\ell_1^2} r_1 \tag{70}$$

where n_1 is the integer characterizing the cavity mode in the x_1 direction.

Relation (69b) expresses the change in $k_1(0)$ due to the fact that the wall takes part in the vibration. The equation can be expressed in the form

$$\Delta k_1 = -\frac{k_1(0)}{\ell_1} \Delta \ell_1 \tag{71}$$

where $\Delta \ell_1 = m_1 / \rho_o$ which represents the thickness of a layer of the contained fluid, which has the equivalent mass per unit area as the stainless steel sheet. Using the previous expression for $k_1(0)$, the corrected k_1 is then given by

$$k_1 = \frac{n_1 \pi}{\ell_1 + \Delta \ell_1} \tag{72}$$

in which the conventional relation for k_1 is employed with the actual ℓ_1 augmented by the correction $\Delta \ell_1$.

An example calculation of the fundamental mode of vibration for cavity No. 2 will serve as an illustration of the application of the above relations. The inside dimensions of the cavity are 12 x 8 x 10 inches, the latter number being the depth. The cavity walls are stainless steel sheets of 24-mil thickness. Using a specific gravity of stainless steel equal to 7.9, the correction $\Delta \ell$ for each wall is 190 mils or 0.19 inch.

The cavity is open on the top and was employed with the water level always 0.25 inch below the rim. The effective cavity dimensions (using $\Delta \ell = 0$ for the free surface) are accordingly 12.38 x 8.38 x 9.94 inches. For the fundamental mode of vibration (n_1, n_2, n_3 being 1, 1, 1 respectively), the effective wave numbers for the cavity are accordingly

$$k_1, k_2, k_3 = \frac{\pi}{12.38}, \frac{\pi}{8.38}, \frac{\pi}{9.94}$$

in units of radians/inch. This yields

$$\sqrt{\sum_{i=1}^{3} k_i^2} = 0.17575\,\pi = \frac{\pi}{5.69}$$

and from the first of relations (66)

$$\omega = 2\,\pi f = \frac{\pi c}{5.69}$$

or

$$f = 0.08787\,c$$

For the temperature and salinity conditions of 60°F and 34 gms/kg, the value of c from standard tables is 4935 ft/sec

and hence

$$f = 5204 \text{ c/s}$$

This value is in good agreement with the experimental results for cavity No. 2.

An estimate of the acoustic loss suffered by radiation into the surrounding air can be determined by assuming that the air load is 42 acoustic ohms (i.e., $r_1 = r_2 = r_3 = 84$ acoustic ohms). The generalized counterpart of (70) is

$$\alpha_i = \frac{\pi}{\rho_o \omega} \frac{n_i}{l_i^2} r_i$$

Combining this with relations (65) yields

$$\alpha_t = \frac{\sum k_i^3 r_i}{\pi \rho_o \sum k_i^2} \tag{73}$$

The latter quantity gives the temporal attenuation rate in neper/sec. The corresponding spatial attenuation factor $\alpha_o = \alpha_t / c$. Using the above relations with the assumed value of r and the previous values of k_i gives $\alpha_o = 1.66$ neper/kyd, which corresponds to 19.2 db/kyd.

This is of the same order of magnitude as the losses determined experimentally for the cavity filled with pure water. The viscous attenuation due to the pure water, for the same size cavity, is only of the order of 0.5 db/kyd as estimated from the relations in the following section.

Cavity with Internal Losses plus Radiation

The theory of a resonant cavity developed in the preceding is only applicable when the fluid is essentially

without frictional losses. An approximate solution can be obtained, if it is assumed that the losses are low. The cavity is, in other words, strongly resonant. The highest attenuation that can be measured with the present equipment corresponds to a cavity Q of 470, and the Q with clean water in the cavity is of the order of 7500, so the losses are actually quite small when compared with electrical resonant circuits.

The wave equation (15) for a viscous fluid is employed in the present analysis. The solution for the components of displacement as given by (45) is still pertinent; however, the expressions for the complex wave numbers and frequency will differ from the previous case. Substitution of (45) in (15) yields

$$\frac{\partial^2 \varepsilon}{\partial t^2} = c^2 (1 - \beta \Omega) \nabla^2 \varepsilon \tag{74}$$

where $c = \sqrt{\lambda_o / \rho_o}$ and $\beta = (2\mu_1 + \lambda_1)/\lambda_o$ as employed previously.

The evaluation of the characteristic equations is formally the same as in the previous case except that c^2 is to be replaced by $c^2 (1 - \beta \Omega)$ in relation (64). Thus the counterpart of (64) is

$$\Omega^2 = c^2 (1 - \beta \Omega) \sum_1^3 K_i^2 \tag{75}$$

The auxiliary relations relating K_i, Ω and the boundary impedances are formally the same as (66), except that the K_i and Ω are now dependent upon β as well as the boundary impedances. However, the form of (66) demands that the first order effect of attenuation on K_i is due to the boundary impedance. Any effect of β will be of second order in respect to K_i. Consequently relations (69) and their counterparts for coordinates x_2 and x_3 are still valid.

The primary effect of the viscous parameter β enters in the evaluation of α_t. By separating relation (75) into its real and imaginary parts and neglecting terms involving β^2, α_t^2 and α_i^2 the following approximate relations are obtained:

$$\text{(a)} \quad \omega^2 = c^2 \sum_1^3 k_i^2$$

$$\text{(b)} \quad \alpha_t = \frac{c^2}{\omega} \sum_1^3 \alpha_i k_i + \tfrac{1}{2} \beta \omega^2 \qquad (76)$$

where k_i and α_i ($i = 1, 2, 3$) are given by relations of type (70) and (72) with appropriate changes in subscripts. Specifically, the allowable values of k_i depend only on the cavity geometry and the equivalent thickness of the walls. The values of α_t depend upon the cavity geometry and the real part of the boundary impedance.

Relations (76) differ from (65) only in the addition of the viscous attenuation term to α_t. It will be noted that the resonant frequency is not influenced by viscosity in the present approximation. Moreover, relation (76b) shows that the effects of internal (viscous) losses are additive in respect to the attenuation coefficient α_t. In other words there is no first order coupling of the internal and external (radiational) attenuation phenomena. This is an important result, since it allows the possibility of evaluating the internal losses in a fluid sample by measuring the total loss and subtracting the radiational loss. The latter is determined experimentally by the calibration tests with a virtually inviscid fluid (air-free, pure water).

It will be noted that relation (76b) is consistent with the result anticipated in the considerations of the acoustic energy decay (page 36). It was shown by a somewhat heuristic chain of reasoning that the exponential decay factor (per unit time) for energy could be expressed in

the form

$$\gamma \frac{cA}{V} + \beta \omega^2$$

where γ is a transmission coefficient which gives the fraction of incident energy flux which leaks through the boundary. The ratio V/A defines a characteristic dimension L for the cavity (V being the volume and A the surface area). Thus the above relation can be written

$$\frac{\gamma c}{L} + \beta \omega^2$$

Bearing in mind that this should correspond to $2\alpha_t$, where α_t is the amplitude decay modulus, it is seen that this is consistent with (76b) provided that

$$\gamma = 2L \frac{c}{\omega} \sum_{1}^{3} \alpha_i k_i \tag{77}$$

The quantity on the right can be shown to be directly proportional to the impedance ratio $r/\rho_o c$ as should be expected provided that the ratio is suitably small. The factor of proportionality depends upon the shape of the cavity and the particular mode of oscillation.

Practical Relations Implied by the Theory

The result (76b) for the temporal decay factor pertinent to a resonant cavity consists of two parts

$$(\alpha_t)_{\text{total}} = (\alpha_t)_o + (\alpha_t)_{ex} \tag{78}$$

where $(\alpha_t)_o$ is the attenuation factor associated with the particular properties of the cavity and $(\alpha_t)_{ex}$ represents excess attenuation associated with the contained fluid.

The above factors, as they stand, represent attenuation in units of neper per unit time. In measurements the reverberation time is determined. This represents the time that it takes the sound level to die down 60 db, measured in seconds. Thus if t_o denotes the reverberation time as measured with the cavity filled with pure water and t_{total} the reverberation time as measured with a sea water sample, then

$$(\alpha_t)_{ex} = 60 \left[\frac{1}{t_{total}} - \frac{1}{t_o} \right] \tag{79}$$

the units being db/sec.

In practice it is the attenuation per unit length along the propagation path which is desired. From the considerations of the plane sound waves it is evident that the conversion to the spatial attenuation factor, α_k, for the fluid is simply $\alpha_k = \alpha_t / c$. For sea water of 34 gms/kg salinity at 60°F c = 1.645 kyd/sec; hence the excess attenuation expressed as db per kyd is given by

$$\alpha_k = 36.5 \left[\frac{1}{t_{total}} - \frac{1}{t_o} \right] \tag{80}$$

This relation has been used in the evaluation of the data.

It is theoretically possible to determine the sound velocity from the resonance frequency, but the geometrical dimensions of the cavity are not very stable, since it is made of thin sheet metal with welded corners. The accuracy of the frequency measurements were only as good as can be obtained by reading the scale on the tone generator, and the determination of c on this basis is not precise. The temperature range encountered was from about 10°C to 20°C, and the sound velocity changes about 2 per cent due to this temperature variation, but it is not known how the presence of plankton may change c. It was therefore decided to use a constant value for c, to be able to give α_k

in units that can be easily interpreted, instead of db/sec.

Some Final Remarks Regarding the Theory

The most general boundary conditions considered required the determination of p and v_n at the boundary. The pressure p was determined from equation 1a, with the simplification that μ_1 and λ_1 were zero. These terms, however, can still be disregarded as long as the viscous part of the pressure tensor is insignificant compared with the elastic part. This same approximation has been used in the preceding analyses.

In the more general case, the velocity at the boundary must now satisfy one further condition, beyond the condition imposed by the acoustical impedance of the boundary. This condition is that the component of the velocity tangential to the boundary must vanish. To satisfy this boundary condition, there must exist a transverse frictional wave in the immediate neighborhood of the boundary, since such waves experience an extremely high attenuation with distance. This will add to the boundary losses, but these are determined experimentally in any event. It must be borne in mind, however, that the reference liquid should have approximately the same shear coefficient μ_1 as the liquid under investigation, and approximately the same sound velocity c.

V. EXPERIMENTAL PROGRAM

OBSERVATIONAL PLATFORM

The equipment described in Section III requires a reasonably stable supporting surface to work properly. It would not be possible to use this equipment on a ship. On the other hand, the time delay suffered if samples were taken at sea and brought back to the laboratory would be highly undesirable.

The NEL Oceanographic Research Tower off Mission Beach, San Diego, is well suited for cavity measurements, and a program was therefore initiated to develop equipment suited for this research facility.[40,41]

The tower is situated 0.8 nautical mile off the shore in approximately 59 feet of water. The shoreline off Mission Beach is completely unobstructed from the influences of the open ocean. The influence from man-made contamination is therefore at a minimum. The main deck of the platform is 24 feet above the water level, and acts as foundation for an instrument house of 13 by 13 feet in plan section. This leaves an outside passageway around the house about $4\frac{1}{2}$ feet wide. Space inside the house was not available, so the instrumentation had to be placed outside in the passageway. The tower is quite stable, but the action of waves on the tower supports causes a slight oscillation. The main influence was from the wind, which often would spoil a reverberation measurement by creating ripples on the surface of the water in the cavity. Measurements were impossible whenever very "noisy" equipment was in use such as compressors and heavy winches, but the cavities worked well when the conditions were favorable.

The present field data collection began May 1960 and continued through the summer until the tower was closed down in September 1960.

The instrumentation on the tower permits a large number of oceanographic variables to be measured. It is neither reasonable nor practically possible to try to correlate every available parameter with the attenuation measurements. In the present experiments the plankton count and oxygen content of the water are regarded as the primary factors. Moreover, these variables together with temperature and salt content describe the state of the sample (at atmospheric pressure) in a direct manner, independent of the source and procedure of sampling.

The viscosity coefficients of the water partially determine the attenuation. It is known that these coefficients are functions of temperature and salinity for clean sea water, but the effect is very small compared with the attenuation measurable with the cavity equipment. The temperature was measured for every sample, but the salinity was not considered. The salinity does not change appreciably around the tower, since there are no fresh-water outflows close by and there is fairly easy exchange with the open ocean water.

Samples were taken anywhere from the surface to the bottom. Some samples would therefore have undergone considerable pressure changes before the measurements. The pressure change would not have any appreciable effect on the sea water itself, but it can well have a marked effect on the suspended particulate matter as well as on the dissolved gases. The sampling depth was therefore recorded for all samples. However, it should be borne in mind that the plankton counts and oxygen content were determined for the sample at atmospheric pressure. The in situ conditions of these variables and the quantitative influence of pressure are a separate problem and beyond the scope of the present study.

The tower is equipped with a hydrophotometer and measurements are recorded as the per cent transmission of that in pure distilled water. The path length of this instrument is $\frac{1}{2}$ meter. Sea water samples at depths between surface and bottom have an up-and-down motion due

to surface waves and internal waves. The hydrophotometer reading will likewise change considerably, and it is not possible to ascribe a very reliable light transmission reading to any particular sample. The readings on the hydrophotometer are a function of particulate matter (including plankton) and air bubbles suspended in the measuring path of the light beam, but there are no functional expressions available describing this relationship. The hydrophotometer readings were recorded when available. However, these measurements are to be regarded purely in the nature of qualitative information about the general nature of the in situ conditions of the region being sampled.

As mentioned earlier, the greatest emphasis in the analysis is placed on the dependence of attenuation on the plankton count and oxygen content as measured from the sample.

EXPERIMENTAL PROCEDURE

Sampling Methods

Surface samples were at first obtained by using a bucket at the end of a line. Deeper water was obtained by using standard Nansen bottles. However, it soon became clear that either method was highly unsatisfactory. It was almost impossible to fill a cavity from the bucket without working a large amount of air bubbles into the water, and it was very slow and cumbersome to obtain enough water with Nansen bottles.

A small submersible centrifugal pump was then procured and mounted on the cart carrying the hydrophotometer. A hose carried the water up to the main deck where the cavities were. The pressure in the discharge line from the pump was approximately 12 psi higher than the hydrostatic pressure at the level from which the sample was taken. Cavitation was therefore not likely to occur.

The discharge of the hose was always kept below the water level in the cavity, and no bubbles were ever observed coming out of the hose. This sampling method was used exclusively in all of the subsequent work, but it was felt that a less "violent" sampling method would be preferable.

Selection of Cavity for Measurements

Five cavities were available for the data collection, as mentioned earlier. It became apparent however, that only cavity No. 2 was suited for measurements on the tower. Cavity No. 1 was too big for one person to handle, considering the rather limited space available. The difficulties encountered when cleaning the walls and stirring the content to insure homogeneity were also considerable. The cavities smaller than cavity No. 2 were likewise difficult to clean because of their small size and also because the walls were not sufficiently flexible.

The influence of the transducers was also marked for cavities 3, 4, and 5 probably partly because of the greater transducer dimensions relative to the wavelength for the cavity. This is also partly because the transducers could not be decoupled to as great an extent as with cavity No. 2, since the thickness of the stainless steel sheet corresponds to a greater fraction of a wavelength.

It was decided to use cavity No. 2 exclusively for the data collection. This implies that it is not possible to deduce very much about the variation of the attenuation with frequency. However, even if the same sample had been used in all five cavities, the frequency range is not great. Moreover, transferring the sample from one cavity to another would undoubtedly have a very marked influence on the properties of the sea water. An attempt was made, however, to get data at different frequencies by measuring the reverberation time of not only the fundamental mode, but also two higher modes. If the coordinate axes 1, 2, 3 are identified with length, width, and depth of the cavity, then the modes measured can be labelled:

$$(n_1, n_2, n_3) = \begin{matrix} (1, 1, 1) \\ (1, 2, 1) \\ (2, 1, 1) \end{matrix}$$

Before a consistent data collection could be undertaken, it was necessary to find a method for keeping the side walls of the cavity clean. Of the several methods which were tried, a squeegee mounted on a thin tube appeared the most satisfactory. This device made it possible to insure absolutely clean walls, with the only drawback that of the unavoidable disturbance in the water.

Evaluation of Oxygen and Plankton

Special precautions were taken in drawing plankton and oxygen samples from the water in the cavity. A 50-ml pipette with the tip removed was used to draw the samples, and it was rinsed clean and thoroughly wetted before each sampling. The plankton was drawn from the center of the cavity, where its influence on the acoustic properties of the sea water would be most pronounced. To avoid the inclusion of water too far removed from the center, only about 1 ounce was drawn. The sample was immediately preserved by adding 2 cc of 40 per cent formaldehyde solution to the sampling jar.

The plankton count was obtained by shaking the sample thoroughly, filling a Sedgwick-Rafter counting cell with the sample, and counting the organisms by 100x in a microscope.

In drawing oxygen samples, great care was taken not to work bubbles into the water at any time. The pipette was allowed to fill by itself without suction, and the tip was touched to the inside of the 0_2 bottle held at a slant, so that the pipette would empty slowly and smoothly. The preservation and titration of the sample followed the standard procedure used in connection with Winkler determination of oxygen. Standard 150-ml oxygen sample bottles with ground glass stoppers were used throughout.

The per cent saturation of oxygen was computed in accordance with reference 42.

Outline of Experiment Procedure

The procedure for taking a measurement can be summarized as follows:

(1) Fill cavity with sample.

(2) Wipe side walls and bottom with squeegee.

(3) Tune generator frequency and the tuning circuit to obtain maximum reading on vacuum tube voltmeter (fig. 4B).

(4) Decouple transducers until barely full reading is obtained on recorder, and with VTVM sensitivity as high as possible.

(5) Start recorder at paper speed chosen (100 mm/sec or 30 mm/sec), and interrupt power from the signal generator.

(6) Tune generator to the two higher modes, repeating steps 3, 4, 5.

(7) Take plankton and oxygen samples, and measure temperature.

(8) Record sampling depth and hydrophotometer reading.

Calibration of Cavity

The cavities were calibrated before they were used on the tower and again after the data collection with no change in their acoustic properties indicated. Visual inspection did not disclose any change in the cavities apart from a slight surface discoloration of the stainless steel sheets.

The calibration was done with the cavities filled with distilled water. The temperature was brought down early

in the morning by adding sufficient distilled water ice, and the calibration was performed while the cavity was heating up. The cavity walls were carefully wiped whenever a desired temperature was reached, and a series of reverberation curves were then taken for different distances, D, between the rim of the cavity and the surface of the water. A series at any one temperature always began with a full cavity, and the walls were wiped only at the beginning of a series. The difference in the water temperature between the beginning and the end of a series was always less than 1°C, and the temperatures given are the average of the series.

The calibration data are given in figures 9 to 14. The attenuation coefficient for the cavity, α_o, is plotted as a function of D and of the resonance frequency f_o. Figures 9 and 10 apply to mode 1-1-1, or the fundamental mode. Figures 11 and 12 correspond to mode 2-1-1 while figures 13 and 14 pertain to mode 1-2-1. Figure 9 shows $\alpha_o(D)$ for different temperatures. There is a discouragingly large spread between the different points, and it appears that the case D equal to $\frac{1}{4}$ inch below the rim is particularly poor. Replotting the same points, but this time using the resonance frequency as the independent variable, led to figure 10. The scatter has to a great extent disappeared. An investigation showed the cause of this behavior to rest with the spacing between the cavity and the supporting table. The cavity is approximately 14 mm above the table, and a quarter wavelength in air is about 18 mm at 5000 c/s. The distance between the table and the cavity could be increased by blocking the cavity supports up, and decreased by inserting a $\frac{1}{4}$ inch aluminum plate between the cavity and the table. It was found that the distance actually improved the cavity Q. Moving the supports as far as $\frac{1}{4}$ inch away from the corners did not affect the losses of the cavity, however.

In regard to the calibration data for modes 2-1-1 and 1-2-1 (figs. 11-14), the attenuation due to the cavity is generally greater than that associated with the fundamental mode (at least for frequencies greater than 5.2 kc/s). In addition, the attenuation varies greatly with frequency,

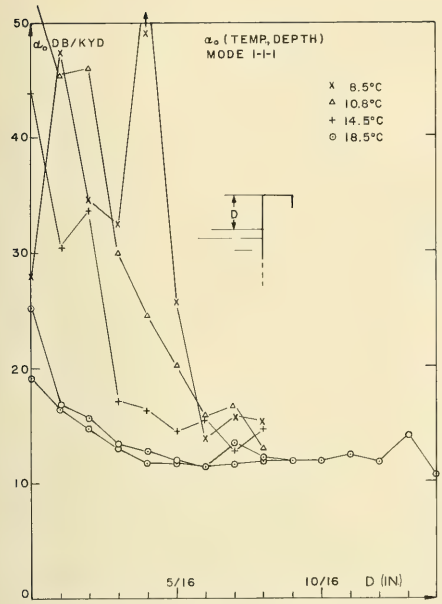

Figure 9. Calibration tests for mode 1-1-1, showing attenuation coefficient (α_o) vs. distance (D) between free surface and cavity sill, using pure water at four different temperatures as indicated.

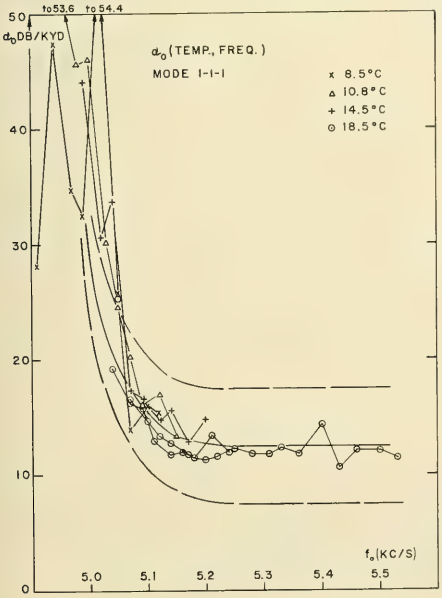

Figure 10. Calibration tests for mode 1-1-1, showing attenuation coefficient of figure 9 replotted vs. the resonant frequency (f_o).

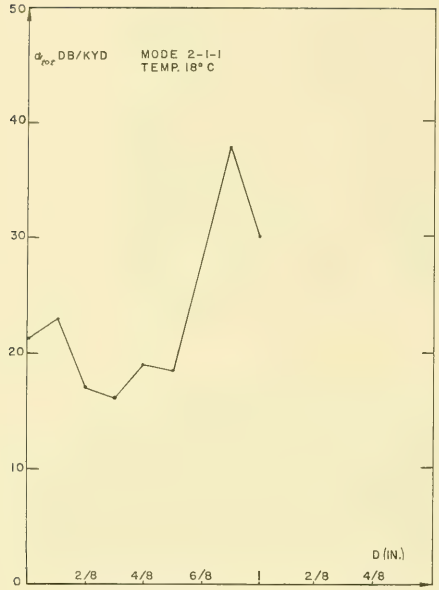

Figure 11. Calibration tests for mode 2-1-1, showing attenuation coefficient vs. D, using pure water at 18°C (no correction for attenuation by the water).

Figure 12. Calibration tests for mode 2-1-1, showing attenuation coefficients of figure 11 plotted vs. resonant frequency f_o. Temperature 18°C.

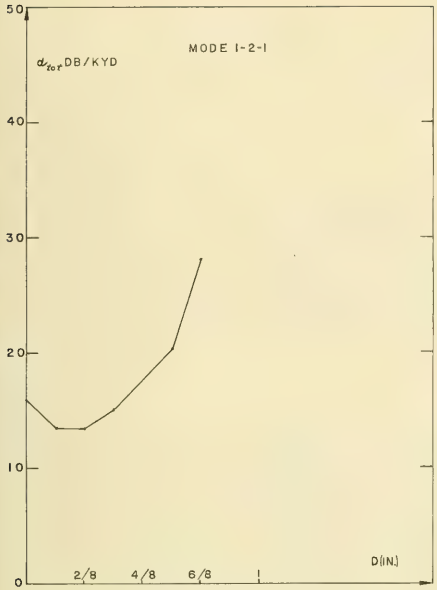

Figure 13. Calibration tests for mode 1-2-1, showing attenuation coefficient vs. D, using pure water at 19°C (no correction for attenuation by the water).

Figure 14. Calibration tests for mode 1-2-1 showing attenuation coefficients of figure 13 vs. resonant frequency.

particularly for mode 2-1-1. The data accumulated for these two modes have therefore not been corrected for the loss in the cavity itself.

The block diagram utilized for the calibrations and the captured bubble measurements were the same as shown in figure 4B, except that a quartz crystal controlled electronic counter was connected in parallel with the output terminals of the generator. The frequency was therefore known with an accuracy of ±1 c/s. The circuit used for the measurements of the sea water samples is identical to that shown in figure 4B.

The glass rod shown in figure 2 is very useful as a probe of cavity modes. Any particular mode can be identified by passing a captured bubble through the cavity. The reading on the VTVM instrument will be a minimum when the position of the bubble coincides with a pressure maximum in the cavity. This method was always used to identify the cavity modes, whenever it appeared necessary. The mode with the lowest resonance frequency is of course always mode 1-1-1.

A few measurements on a captured air bubble are included as an illustration of the capability of the cavity used for the data collection. The original reverberation curves obtained from the Brüel and Kjaer recorder are shown in figures 5 to 7, and the results(discussed in a later section)are plotted in figure 15. It should be noted in passing that the diameter of the bubble for each test was estimated by comparison with the divisions of a metric scale, the bubble being held by the glass rod. The accuracy is accordingly rather poor.

Character of the Reverberation Curves

The reverberation curves do sometime show evidence of "double" moding. The reverberation level diminishes through the first 10-15 db at a faster rate than encountered

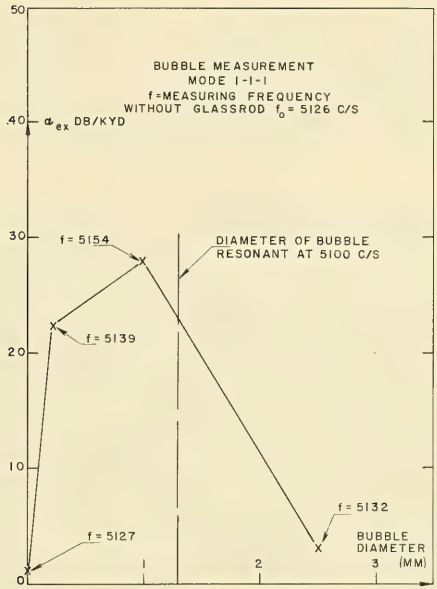

Figure 15. Excess attenuation coefficient for mode 1-1-1 due to presence of air bubble vs. bubble diameter (using data of fig. 5, 6, 7).

later on. If the output from the receiving hydrophone is recorded as a function of frequency when a double mode prevails, it is always found that there are two resonance peaks close together in frequency. The peak with the lower level is always narrower in bandwidth than the peak with the higher level. This would imply that the lower peak corresponds to a normal mode more loosely coupled to the transducers, but with a smaller damping than the higher peak. It was usually possible to eliminate the mode with higher damping by altering the effective coupling between the transducers and the cavity. The reverberation time measured on the mode with lower damping does not change by this procedure. The mode with the longest reverberation time was therefore used in the few cases where the above corrective method did not work. However this was

done only if the reverberation trace displayed a straight part of at least 25 db. Otherwise it could not, with certainty, be differentiated from the part where the reverberation curve merges into the noise level.

Possibility of Cavitation

The maximum sound pressure level in the cavity is not known, but it will be a function of the cavity Q. The highest sound pressure is found in the center when the 1-1-1 mode is utilized, and in the corresponding points for the higher modes. The possibility therefore exists that the water may be cavitating in the pressure maximum or maxima. The earphones (fig. 4B) were therefore always used when a measurement was taken, and it was never possible to detect any indication that cavitation occurred. Reverberation curves taken in rapid succession always gave essentially the same result, and they were always straight with the above mentioned exception. It was concluded that the results were not explainable as being caused by cavitation.

Anomalous Observation

A peculiar phenomenon occurred twice during the data-taking period. The cavity had been filled with plankton-rich water and left standing. No measurements were completed because a brisk wind created fairly large ripples on the free water surface and made the water in the cavity turn over slowly. After 5 to 10 minutes the plankton had disappeared from the water, and a few strings of gelatinous matter, 3-5 mm in diameter and 20-50 mm long, were found floating in the surface. The gelatinous matter had a very large number of air bubbles embedded in it, and later microscopic investigations showed it to contain large quantities of chlorophyll. This has some bearing on a possible source of bubbles which is explored in the discussion to follow.

DISCUSSION OF RESULTS

Accuracy of Attenuation Coefficients

The greater part of the data, especially the part which showed large attenuation, was obtained at frequencies above 5.1 kc/s, and the change in cavity loss is fairly small in this range. The few points taken at frequencies lower than 5.1 kc/s were obtained for the cold oceanic water, and these samples had a very low attenuation.

The values of the attenuation rate indicated in the calibration curve of figure 10 were computed from the relation

$$\alpha_o = \frac{36.5}{t} \text{ db/kyd}$$

The reverberation time t was obtained from recordings like those shown in figures 5 to 7 by matching a straight black hairline, engraved in a piece of clear plastic, with the reverberation curve. By having the curves read several times by different observers, it was found that the accuracy with which the reverberation time could be read was:

$$\Delta t \lesssim \pm 0.02 \text{ sec for } t \lesssim 1 \text{ sec or } \alpha_o \gtrsim 36.5 \text{ db/kyd}$$

and

$$\Delta t \lesssim \pm 0.05 \text{ sec for } t \gtrsim 3 \text{ sec or } \alpha_o \lesssim 12 \text{ db/kyd}$$

The relationship between Δt and $\Delta\alpha_o$ can be obtained by differentiation of the above relation for α_o. This yields

$$\Delta\alpha_o = \pm \frac{\Delta t}{36.5} \alpha_o^2$$

This relation gives the following:

$$\Delta\alpha_o \cong \pm 0.2 \text{ db/kyd for } \alpha_k = 12 \text{ db/kyd}$$

$$\Delta\alpha_o \cong \pm 1 \text{ db/kyd for } \alpha_k = 40 \text{ db/kyd}$$

$$\Delta\alpha_o \cong \pm 20 \text{ db/kyd for } \alpha_k = 200 \text{ db/kyd}$$

The above computation considers only the accuracy with which the reverberation curves can be read. Spurious resonances caused by inhomogeneities in the cavity equipment or in the liquid sample will give rise to additional inaccuracies in the measurements. The encircled points in figures 9 and 10, marked 18.5°C, were recorded on two different days, and show that the measurements can be repeated within a few db, at least in the part of the curve of interest for the data reduction. Inspection of figure 10 shows that the measured points are essentially contained in the interval $\Delta\alpha_o = \pm 5$ db/kyd for the part of the calibration curve above 5.1 kc/s, which is the part of greatest interest for the data.

The excess attenuation, α_{ex} is computed as the difference between α_{tot} and α_o, and $\Delta\alpha_{ex}$ must therefore be larger than $\Delta\alpha_o$. It has been assumed that excess attenuation is present in a sample, when the measured value for α_{ex} is greater than 10 db/kyd.

Remarks Concerning the Bubble Measurements

The original measurements on a captured bubble are shown in figures 5 to 7. The transducers were adjusted with no glass rod in the cavity and not changed during the measurements. The value for α obtained by this setting was used as the value of α_o, and the excess attenuation,

α_{ex}, was determined on this basis. The attenuation with the flooded glass rod suspended in the center of the cavity was the same as without the glass rod, within the accuracy of the measurements. By sighting along the reverberation curves in figures 5 to 7, it can be seen that they are not absolutely straight. The straight part with the smallest attenuation is, however, long enough to give a reasonably accurate determination of the reverberation time. The points obtained have been plotted in figure 15, and the vertical dashed line in this figure corresponds to the diameter of a free bubble resonant at 5100 c/s. The glass rod will undoubtedly change the resonance frequency as well as the attenuation from the corresponding values for a free bubble, but the agreement is still quite good.

A vibrating bubble radiates a spherical sound field, which will represent a scattering loss if the bubble is situated in a plane progressive sound field. This same spherical sound field will not cause a loss when measurements are carried out in a cavity with the bubble suspended in the center, but it will cause a change in the resonance frequency of the cavity.

The Sea Water Data

The attenuation values as evaluated from the measurements on the sea water samples are contained in figures 16 to 32. The group 16 to 20 pertain to measurements for mode 1-1-1; group 21 to 25, to mode 2-1-1; and group 26 to 30, to mode 1-2-1. It will be recalled that the three different modes correspond to the following frequency bands: 5.0 to 5.5, 6.5 to 6.7, and 7.8 to 7.9 kc/s (the exact value of the resonant frequency for each mode being dependent mainly upon the depth of water). Figure 31 illustrates the variation of attenuation with time for a series of samples taken over a period of about 16 hours. Figure 32 is a sequence of measurements taken in rapid succession for given samples over a period of about 100 minutes.

The three groups of five figures corresponding to the different frequency modes are arranged in the same order. The first graph in each group is a scatter diagram of attenuation versus relative oxygen content (as per cent saturation). The remaining four graphs in each group show the attenuation versus particle count for the following particle types: Gonyaulax, Peridinium, broken cells (with chlorophyll) and all particles collectively. As noted earlier, the attenuation is given in terms of excess relative to that of the cavity for the first group only (mode 1-1-1). The total attenuation is given in the second two groups in view of the somewhat uncertain behavior of the cavity attenuation for the modes 2-1-1 and 1-2-1.

The most striking thing one observes in these results is the large scatter of value of attenuation, a feature which seems to be inherent in respect to a complex fluid mixture like sea water - whose properties cannot be uniquely defined in terms of temperature, salinity, and pressure alone. The graphs indicate that even oxygen content and particle count are insufficient as additional degrees of freedom for establishing a reproducible relation for attenuation. It is evident that one is confronted with the problem of a random variable in dealing with attenuation in sea water. However, it is tempting to anticipate that the statistical behavior of the attenuation bears some definite relation to the statistics of the particulate matter, oxygen content, etc. There is some evidence for this in the graphs shown here, particularly those indicating attenuation versus per cent saturation with oxygen. However, in view of the rather limited sample of data, there has been no attempt to carry through a detailed statistical analysis.

Some of the scatter in the present measurements may be related to the method of sampling, effects of stirring, and other factors characterizing the experimental procedure. These possibilities are discussed below.

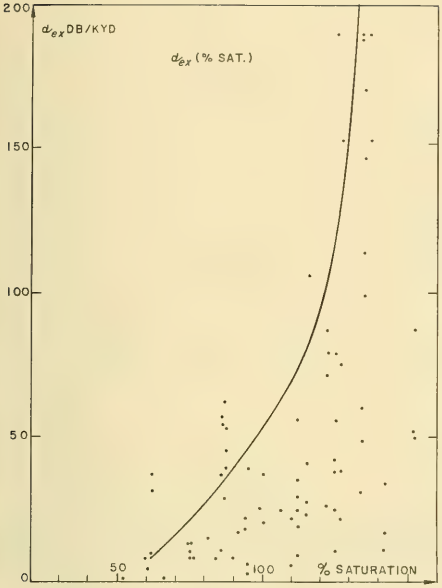

Figure 16. Excess attenuation coefficient for mode 1-1-1 vs. per cent of saturation with oxygen, based on measurements with sea water.

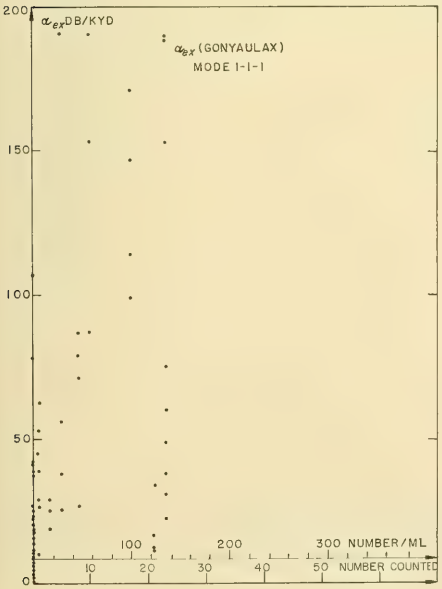

Figure 17. Excess attenuation coefficient for mode 1-1-1 vs. concentration of Gonyaulax expressed as number per milliliter.

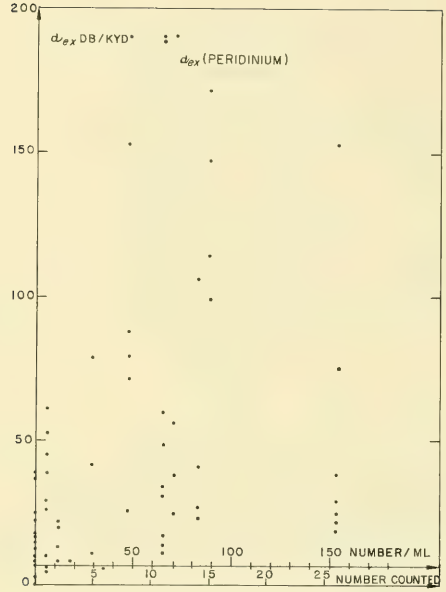

Figure 18. Excess attenuation coefficient for mode 1-1-1 vs. concentration of Peridinium.

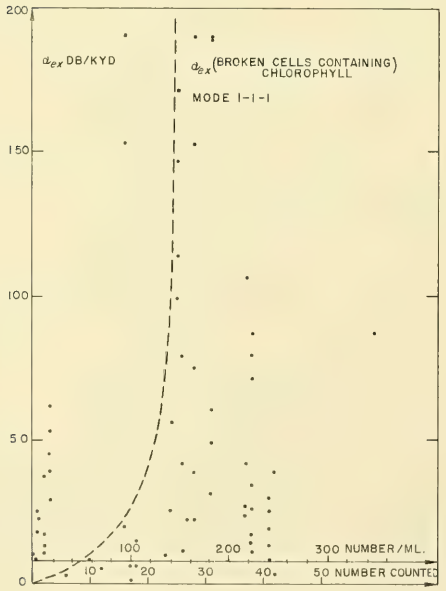

Figure 19. Excess attenuation coefficient for mode 1-1-1 vs. concentration of broken cells which contained chlorophyll.

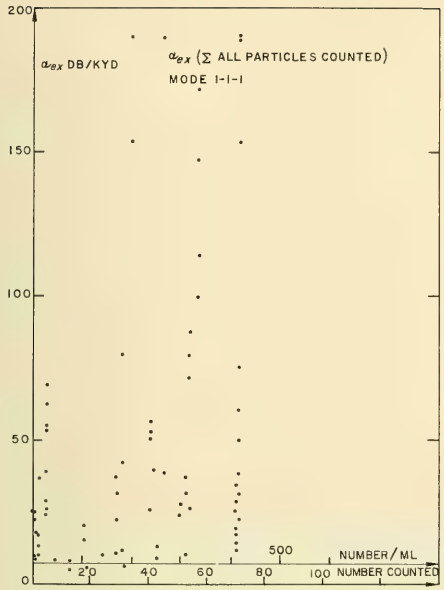

Figure 20. Excess attenuation coefficient for mode 1-1-1 vs. concentration for all organic particulate matter which was counted.

Figure 21. Total attenuation coefficient for mode 2-1-1 vs. per cent of saturation with oxygen (no correction made for cavity attenuation).

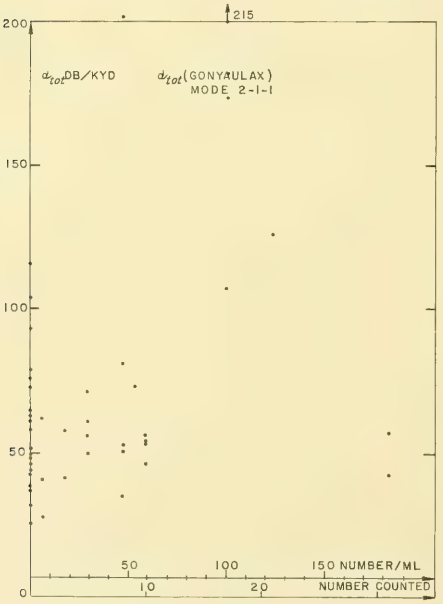

Figure 22. Total attenuation coefficient for mode 2-1-1 vs. concentration of Gonyaulax.

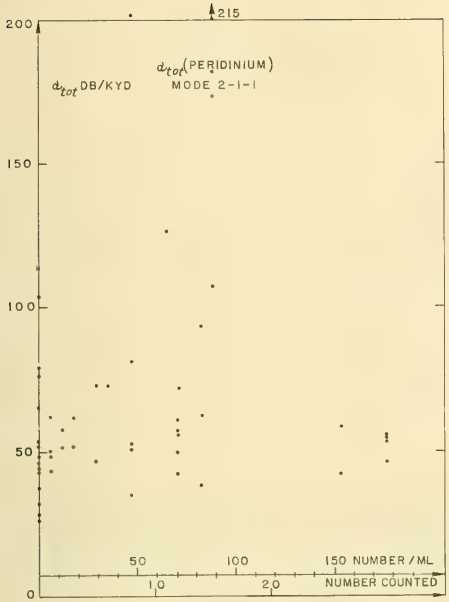

Figure 23. Total attenuation coefficient for mode 2-1-1 vs. concentration of Peridinium.

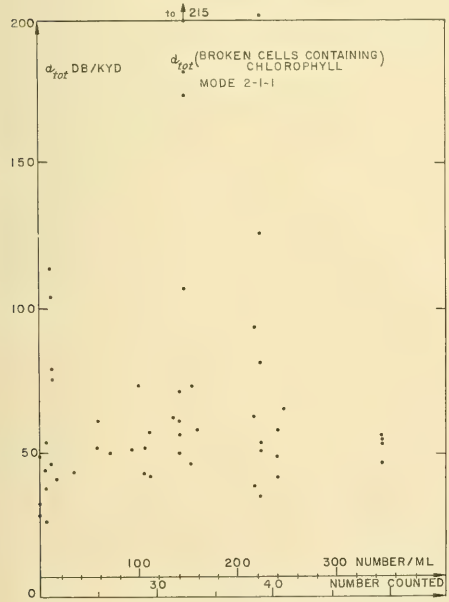

Figure 24. Total attenuation coefficient for mode 2-1-1 vs. concentration of broken cells which contained chlorophyll.

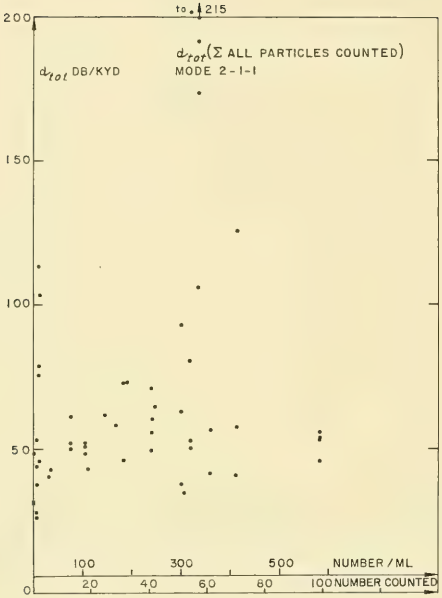

Figure 25. Total attenuation coefficient for mode 2-1-1 vs. concentration for all organic particulate matter which was counted.

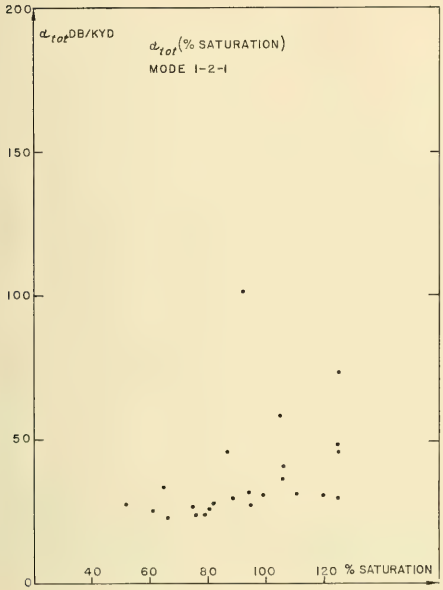

Figure 26. Total attenuation coefficient for mode 1-2-1 vs. per cent of saturation with oxygen (no correction made for cavity attenuation).

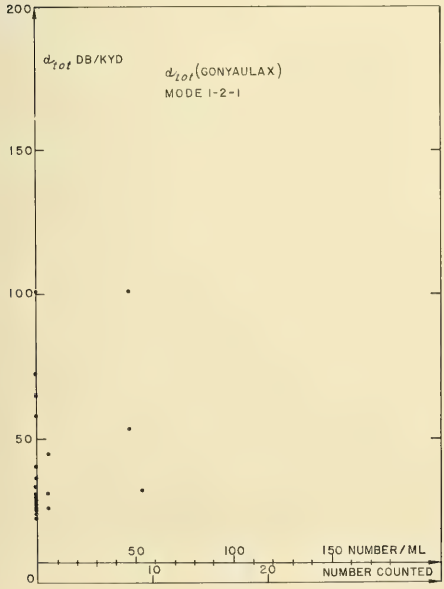

Figure 27. Total attenuation coefficient for mode 1-2-1 vs. concentration of Gonyaulax.

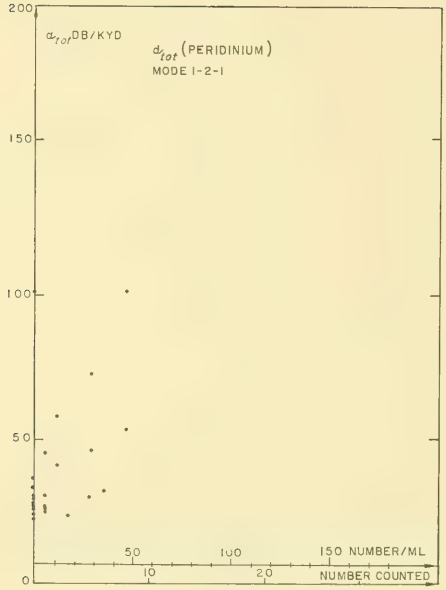

Figure 28. Total attenuation coefficient for mode 1-2-1 vs. concentration of Peridinium.

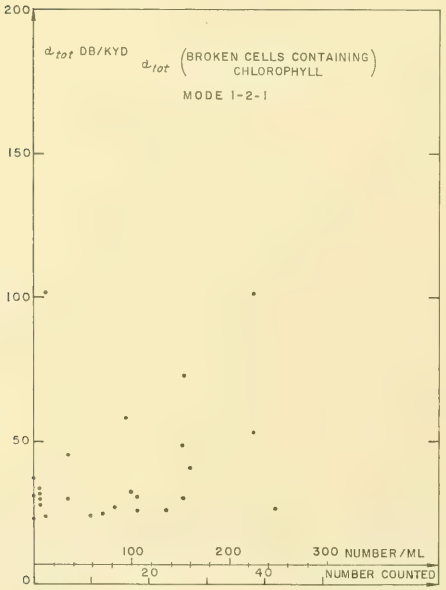

Figure 29. Total attenuation coefficient for mode 1-2-1 vs. concentration of broken cells which contained chlorophyll.

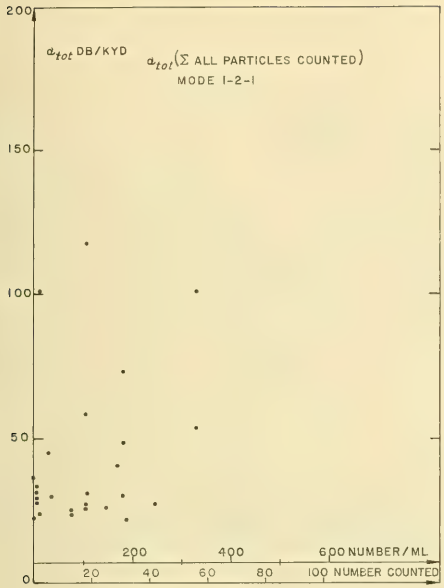

Figure 30. Total attenuation coefficient for mode 1-2-1 vs. concentration for all organic particulate matter which was counted.

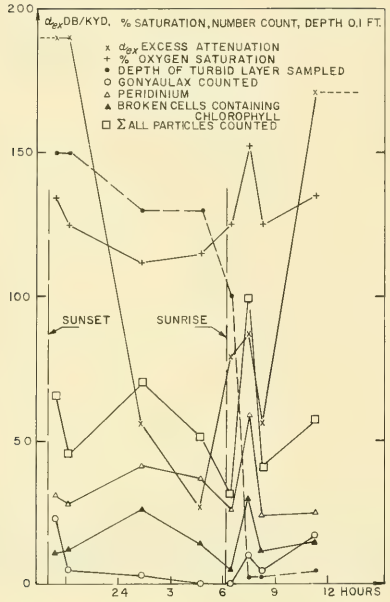

Figure 31. Serial sequences of attenuation, oxygen content, and depth of turbid layer taken during the night of 2 August 1960.

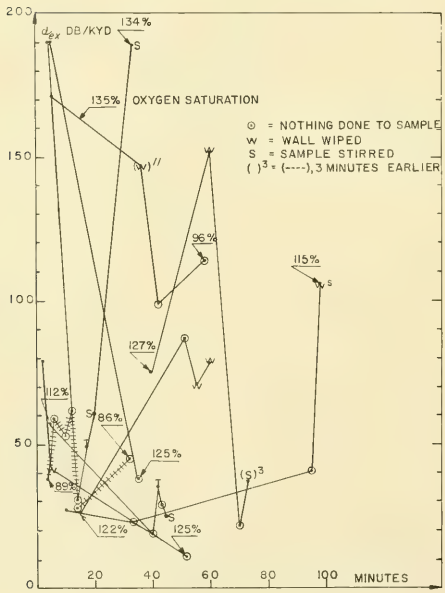

Figure 32. Rapid serial sequence of attenuation showing the effects of stirring and other variables.

Effect of Stirring

Some observations can be made on the basis of figure 32. Even very gentle stirring always increases the excess attenuation, if any is present at all. The sample was always stirred very thoroughly when collected, due to the method of collection by pumping from the sampling depth. Accordingly, the largest attenuation was usually measured immediately after sampling. Different degrees of stirring were tried after the samples were collected, ranging from a thorough stirring with the squeegee to a very gentle stirring with a thermometer. Care was taken not to work any air bubbles into the water when stirring with the thermometer, and the organic material that sometimes settled down to the bottom of the cavity was never disturbed by this action. The attenuation would usually decrease with time, if the sample was not disturbed in any way, but there was almost always residual attenuation of 20 to 30 db/kyd, when the sample had possessed appreciable attenuation initially.

Bubbles did sometimes appear on the sides of the cavity, but wiping them off generally increased rather than decreased the attenuation, presumably due to the unavoidable stirring of the sample. On a few occasions bubbles were observed floating close to the center of the cavity and very large attenuations were measured under these circumstances. Only samples for which no air bubbles could be seen (in the presence of a strong light beam) have been included in the data collection. This limits the possible bubbles to 0.1 mm or less, the largest observable diameter being somewhat dependent upon the kind and amount of suspended matter. Reverberation curves taken in rapid succession give the same value for the reverberation time. It may therefore be assumed that a single measurement of attenuation does not change the acoustic properties of the sample noticeably, but it does not assure that the sample is unaffected by a sound field sustained over an appreciable time.

Effect of Plankton

The attenuation as a function of the plankton content is shown in figures 17 to 20 for the fundamental mode. Two groups of organisms were dominant during the bloom, the dinoflagellate Gonyaulax polyedra (fig. 17) and dinoflagellates of the genus Peridinium (fig. 18). The attenuation in figure 19 has been plotted as a function of the remaining particulate matter containing chlorophyll. Finally, figure 20 gives the sum of the counts in the previous three figures.

The plankton samples had a volume of 1 ounce. The count was performed by first shaking the sample well, and then, using an eye dropper, filling a Sedgwick-Rafter counting cell with a portion of the sample. The dimensions of the chamber are 50 x 20 x 1 mm, and the volume contained is therefore 1 cm^3 (or 1 ml). The count was accomplished at 100 power with a microscope equipped with a Whipple micrometer disk. All the particles within the horizontal lines of the disk were counted during three complete passes in the length direction of the chamber. The calibration showed that the number obtained should be multiplied by 5.9 to give the number of particles per ml. It should be noted that only a small fraction of the particulate matter present was accounted for by the described procedure.

Influence of Sampling Methods

The rather poor correlation of attenuation and plankton count might well be attributed to nonrepresentative sampling. Plankton determinations for biological investigations are often accomplished by towing a plankton net at a chosen depth for a given time. The count can then be performed as described above. However, the accuracy will be much greater since all of the plankton from the large volume of water swept out by the net will be concentrated in a small sampling jar. This method was attempted during the present investigation by letting the discharge from the pump

flow through a plankton net. At the same time the water flow was recorded in liter/min. However, it was evident that a large number of particles went through the bolting silk. The finest netting available was No. 25 with an aperture of 65μ, and the average diameter of Gonyaulax polyedra and Peridinium are 50μ. Moreover, there was no assurance that the plankton count in the pump water would remain constant, since the plankton-rich layer was known to move up and down due to the surface wave action. A count accomplished by this means would therefore not necessarily be representative of the water in the cavity.

Effect of Oxygen Content

Examination of figures 16, 21, and 26 shows that the high attenuations are intimately connected with a high content of oxygen. The highest concentration of phytoplankton was usually found in a well defined layer which varied between the surface and a depth of 20 feet. The oxygen produced by photosynthesis of the phytoplankton can be at saturation under a total pressure well above the atmospheric pressure. It is therefore understandable that the water samples can be supersaturated with oxygen when placed in the cavity at atmospheric pressure. No determination of the nitrogen content was attempted since there is no simple chemical procedure available. A gasometric method must be used and the equipment required was not available, nor could it have been utilized due to the limited space available on the tower.

Dissolved gas has very little effect on the sound propagation in water, as already noted.[33,37] Gas in the form of bubbles does, however, have a marked influence on the sound propagation. Accordingly the high oxygen content indicates that bubbles clearly must be considered in the evaluation of the data.

Free bubbles have a short life in a small sample of a liquid which contains no particulate matter.[36,38] Never-

theless, it has been suggested that bubbles can still be present.[41] A bubble of equilibrium size must satisfy the following equation:[36,43]

$$p_v = p_o + \frac{2T}{r}$$

where

p_v = Pressure due to dissolved gas and water vapor

p_o = Hydrostatic pressure

T = Surface tension

r = Radius of bubble

The last term caused by the surface tension can be neglected when the radius of the bubble is large. The partial pressure of the dissolved gases and the water vapor must then balance the hydrostatic pressure. Equilibrium bubbles are therefore only possible close to the surface. However, these bubbles are unstable. A bubble slightly larger than the equilibrium size will continue to grow since the term due to the surface tensions gets smaller with increasing diameter. These bubbles will soon rise to the surface and disappear. A bubble smaller than equilibrium size will be forced into solution due to the increasing pressure from the surface tension. Bubbles have been utilized in the past in the form of bubble screens,etc., but the bubbles must be produced continually for as long as the effect is desired. It was observed on a few occasions that small bubbles were stabilized in the water by adhering to particulate matter. This partly increased the effective surface of the bubble and thereby slowed its rate of rise to the surface and partly added mass to the bubble counteracting the buoyant force. Samples in which this occurred showed a large attenuation, and the results are not included in the data presented.

Bubble Nuclei

Pure water without any air bubbles has a very high tensile strength.[36] This is in stark contradiction to the behavior of natural fresh or salt water. This discrepancy is usually explained by the presence of gas nuclei in any naturally occurring water mass. The above equation determining the radius of an equilibrium bubble can be considered as the criterion distinguishing bubbles and nuclei. Bubbles smaller than the critical size must somehow be stabilized, or they would soon go into solution. The only agent capable of doing so seems to be particulate matter such as dust.* Filtering or centrifuging are capable of removing the nuclei. This fact can be considered as substantiation of the above viewpoint. Gas nuclei can be removed by applying high pressures to the sample, thereby forcing the small air masses into solution.

The dividing line between nuclei and bubbles will obviously change with the hydrostatic pressure. Nuclei close to the critical size may grow into bubbles, if p_0 is reduced. This is precisely what happens when the sample is pumped up into the cavity.

The very high attenuations measured shortly after sampling, or after the samples were stirred, can perhaps be explained by the development of bubbles which were too small to be seen by direct visual observation. The attenuation remaining after the sample was left undisturbed and also the attenuation measured for nonsaturated water is difficult to explain as an effect of bubbles. It may be remarked in passing that the method of wiping the cavity walls seemed to be quite efficient in removing at least the larger nuclei, since bubbles rarely developed on the sides after a thorough wiping, even though the water was strongly supersaturated.

---

*Ref. 36, p. 95-97

Losses Due to Bubbles

A large amount of work has been done on the problem of the sound attenuation introduced by bubbles.[4,19,34,43,44] The most recent experimental evidence substantiates the notion that the thermal, radiation, and viscous losses adequately describe the attenuation of a bubble vibrating close to its resonance frequency.* It is usually assumed that the effect of bubbles much smaller than the resonance size, corresponding to the measuring frequency, is very small. However, the following discussion indicates that this conclusion may not always be justified.

When the glass rod in the captured bubble experiment was moved around close to the center of the cavity, it was found that the attenuation caused by the bubble was substantially constant provided that the bubble was within a distance of approximately 2 cm from the center. Now suppose the bubble is divided into many smaller bubbles with the same total volume as the single bubble and distributed within 2 cm from the center of the cavity. It must be expected that the resonance phenomenon is basically unchanged. The attenuation caused by the air volume, however, will have changed in a marked degree. The reradiated sound will not contribute to the total loss by cavity measurements, in accordance with the behavior of the single bubble. The viscous losses will be the same or perhaps somewhat larger, since the motion in the water is essentially unchanged except in the immediate neighborhood of the bubbles. The thermal losses will be considerably smaller, since the air in the small bubbles will be almost at the same temperature as the water throughout a wave cycle. The thermal loss of a resonant bubble arises if the disturbance of the gas is neither adiabatic nor isothermal; in this case there must be a phase difference between the acoustic pressure and the particle velocity.

---

*Private communication from Dr. D. E. Andrews, NEL.

There are, however, at least two other sources of loss experienced by a bubble: diffusion of gas and evaporation of water vapor into and out of the bubble during the acoustic cycle. It was not possible to find any investigation of these losses in the literature, presumably because the main interest in the past has been centered on bubbles close to resonant size. Moreover, the resonant bubbles are adequately described by their viscous, thermal, and radiation losses. However, for a given total volume of gas phase within a sample, the surface area available for diffusion and evaporation is inversely proportional to the radii of the bubble. Accordingly one should expect a greater effect due to diffusion and evaporation for the nuclei. The theory of the growth of an air bubble in a sound field by diffusion processes has been investigated in a recent paper[45] and provides a possible approach to the problem of determining energy losses. Reference may also be made to an experimental paper concerned with ultrasonic cavitation traceable to the growth of air nuclei.[46]

Particulate Matter as a Source of Nuclei

The greatest part of the particulate matter in the samples was undoubtedly of organic origin. The question therefore arises whether organic material can produce bubble nuclei and also act as the stabilizing center for a nucleus.

The evidence found in the literature indicates that air bubbles are almost never found in living cells.[47] Bubbles may form, however, if a cell is injured by pinching or cutting and then exposed to reduced pressure. Bubbles may form inside a cell even though the cell wall is not broken by being pinched and they may form in a different place than the pinched spot. This is explained by the unavoidable twisting strains set up in the cell material when manipulated.[47]

There is still another possibility that not only will explain the above experiments, but also the observations

made in connection with the present work. Plant cells have, as a rule, a cell wall that completely encloses the living protoplasm. The pressure in the protoplasm can therefore be considerably higher than the pressure outside of the cell. Oxygen is continually being produced when the plant builds up organic material by photosynthesis. The excess pressure in the protoplasm will increase the saturation level required in the cell to make it possible for a nucleus to grow into a bubble.

Both Gonyaulax polyedra and Peridinium have cell walls in the shape of very elaborate testa that completely enclose the living cell. Nuclei produced de novo by the photosynthetic process will therefore not develop into bubbles under normal circumstances. If the outside pressure is reduced rapidly, such as occurs when the water is pumped up into the cavity, it seems reasonable that bubbles may sometimes develop and make the organism explode. This would explain the two instances where strings of gelatinous material were found floating in the surface of the cavity. Pinching a cell will stretch the cell wall and thereby relieve the inside pressure. Cutting the cell wall will of course have the same effect. If a plant cell dies, it can act as center for bubbles, and the dead cell must consequently contain nuclei. The excess pressure in the cell is connected with the life processes, and will presumably disappear when life ceases. The cell wall will often be broken by death and expose the cell content, and the effect of any nuclei in the protoplasm will therefore be at a maximum.

A recent paper[3] is concerned with the absorption of ultrasonic acoustic waves in water containing algae in suspension. The results given indicate that a very substantial volume viscosity could be attributed to the algae. However, the measuring frequencies were so high (15-27 Mc/s) that no reliable deductions can be made with respect to the present results.

The data presented in this investigation indicate that a relationship may exist between broken cells and the attenuation measured. A very clear-cut correlation could

not be expected, since nothing is known about the length of time required for decaying plant material to stabilize nuclei, nor about the possible production of new nuclei due to the decay processes.

The observations presented here are in many ways similar to the description given by Skudrzyk.* The explanation presented in this reference is based on a continuous production of bubbles, but the experiments were performed at frequencies of the order of 100 kc/s. Bubbles close to resonance will have such a small diameter that it is difficult to verify by visual inspection whether bubbles of this size are present. A frequency of 100 kc/s corresponds to about 0.065 mm diameter.

Serial Sequence of Measurements

One series of measurements was taken through the night of 2-3 August 1960, in an attempt to identify variables of importance to the sound attenuation other than the oxygen content and the count of particulate matter (fig. 31). The samples were taken in the layer of lowest light transmission as indicated by the hydrophotometer. Changes in the different counts reflects not only changes in the density of the layer with highest turbidity, but also the influence of surface waves and internal waves during the sampling period. These changes must therefore be interpreted with some caution.

The samples are supersaturated with oxygen at atmospheric pressure, and the change in concentration through the night is not very great. The upper 15-20 feet were supersaturated through the whole series, and there was no pronounced layer of maximum oxygen concentration. The layer of maximum oxygen content did not coincide with the layer of maximum turbidity.

---

*Ref. 4, p. 869-870

The correlation between the sound attenuation and the variables shown in figure 31 is very poor. The attenuation goes down from its high daytime value to about 30 db/kyd at night, but this value is still significantly higher than the attenuation of pure sea water, and corresponds to the values obtained when a sample was left standing in the cavity.

This behavior can be understood if it is postulated that the plankton produces oxygen nuclei during the daytime hours only. During the dark period the nuclei disappear either because their stability in time is limited, or perhaps because they are carried to the surface by convection currents where they develop into bubbles and escape.

VI. SUMMARY AND CONCLUSIONS

PRIMARY RESULTS

Sea water without suspended particulate matter showed no excess attenuation when compared with distilled water. This is in agreement with earlier work performed at higher frequencies, within the measuring accuracy of the equipment utilized. Nearshore water with high oxygen content and with suspended particulate matter showed excess acoustic attenuation in the full range of the measuring equipment, i.e., from 10 to 200 db/kyd. The largest attenuations were measured for water supersaturated with oxygen, but excess attenuation was experienced even when the oxygen content was only 65 per cent of the saturation value.

The comparison of excess attenuation with suspended particulate matter (primarily plankton) and oxygen content does not indicate a clear-cut correlation, but does suggest the trend indicated above. Perhaps the most striking feature of the measurements is the large range of attenuations which can exist in samples whose gross properties appear to be quite similar.

On the other hand the time sequence of attenuation followed a definite pattern. Whenever any significant amount of attenuation was measured, it would always increase when the sample was stirred. The highest attenuations were consequently usually measured immediately after sampling. The greater part of the excess attenuation, however, would disappear when the sample was left undisturbed, but an excess attenuation of 20 to 30 db/kyd almost always remained even after long periods of time (several hours).

A bubble resonant at 5.2 kc/s will have a diameter of approximately 1.2 mm and is easily visible. It is concluded that the attenuation is not caused by bubbles close to resonance, but may have been caused by much smaller

bubbles or nuclei. It seems likely that the large excess attenuations following stirring are caused by very fine bubbles, when the water is supersaturated, but the attenuation remaining after periods without disturbance may be caused by nuclei. These nuclei may either be stabilized by dead particulate matter, or perhaps inside of living phytoplankton. There is evidence that plankton, at least under certain conditions, do contain nuclei.

The importance of the above considerations in the evaluation of the transmission anomalies encountered in the ocean remains to be seen. Vertical currents are known to exist in nearshore areas, and the pressure changes created may well result in bubble growth when a water mass is brought close to the surface. It was observed at two occasions that bubbles could be stabilized by particulate matter, and there is reason to believe that this phenomenon also takes place in nature. Bubbles stabilized in this manner may again be carried down and cause some of the anomalies observed.

SUGGESTIONS FOR FUTURE STUDIES

Little is known of the acoustic properties of water containing a large number of air bubbles much smaller than resonance size. Future work must therefore include an investigation of small bubbles and nuclei, before a full understanding of sea water measurements can be expected. Special attention must be given to the influence of plankton, since nuclei inside a living cell may have an especially marked effect due to the surrounding organic matter. Only when these problems have been answered satisfactorily is it to be expected that the acoustic properties of plankton itself can be ascertained.

Cavity methods are well suited for most phases of this work. Single bubbles may be created in the center of a cavity around a fine platinum wire by means of electrolysis. This method has been utilized in the past for

measurements on resonant bubbles. Hard-wall spherical cavities may be particularly suited since the losses due to the cavity are as small as possible and the influence of a single very small bubble must be expected to be slight.

To determine the effect of nuclei contained in plankton may require that pure cultures be raised in the laboratory so that the conditions under which the plankton is growing can be established precisely. On the other hand it may be possible to show by much simpler means that plankton at least sometimes contain nuclei by exposing samples of sea water to a vacuum and examining the water microscopically before and after applying the vacuum. In this fashion it may be possible to show with certainty that a pressure reduction at times can cause plankton cells to explode and to conclude that they contain nuclei.

REFERENCES

1. Horton, J. W., Fundamentals of Sonar, 2d ed., United States Naval Institute, 1959

2. Hueter, T. F. and Bolt, R. H., Sonics; Techniques for the Use of Sound and Ultrasound in Engineering and Science, Wiley, 1955

3. Meister, R. and St. Laurent, R., "Ultrasonic Absorption and Velocity in Water Containing Algae in Suspension," Acoustical Society of America. Journal, v. 32, p. 556-559, May 1960

4. Skudrzyk, E., Die Grundlagen der Akustik, Springer, 1954

5. Hashimoto, T. and Kikuchi, Y., "Ultrasonic Propagation Measurement in Sea Water Up to 400 kc," Acoustical Society of America. Journal, v. 29, p. 702-707, June 1957

6. Murphy, S. R. and others, "Sound Absorption at 50 to 500 kc from Transmission Measurements in the Sea," Acoustical Society of America. Journal, v. 30, p. 871-875, September 1958

7. Sagar, F. H., "Comparison of Experimental Underwater Acoustic Intensities of Frequency 14.5 kc with Values Computed for Selected Thermal Conditions in the Sea," Acoustical Society of America. Journal, v. 29, p. 948-965, August 1957

8. Chesterman, W. D. and Gibson, M. J., "An Instrument for Recording Changes of Sound Velocity in the Sea," Acustica, v. 8, p. 44-52, 1958

9. Glotov, V. P., "Reverberation Tank Method for the Study of Sound Absorption in the Sea," Soviet Physics: Acoustics, v. 4, p. 243-248, July-September 1958

10. Naval Research Laboratory Report 4439, Accuracy of Ultrasonic Interferometer Velocity Determinations, by V. A. Del Grosso and others, 6 December 1954

11. Kurtze, G. and Tamm, K., "Measurements of Sound Absorption in Water and in Aqueous Solutions of Electrolytes," Acustica, v. 3, p. 33-48, 1953

12. Musa, R. S., "Two-Crystal Interferometric Method for Measuring Ultrasonic Absorption Coefficients in Liquids," Acoustical Society of America. Journal, v. 30, p. 215-219, March 1958

13. Greenspan, M. and Tschiegg, C. E., "Speed of Sound in Water by a Direct Method," Journal of Research of the National Bureau of Standards, v. 59, p. 249-254, October 1957

14. Tschiegg, C. E. and Hays, E. E., "Transistorized Velocimeter for Measuring the Speed of Sound in the Sea," Acoustical Society of America. Journal, v. 31, p. 1038-1039, July 1959

15. Markham, J. J. and others, "Absorption of Sound in Fluids," Reviews of Modern Physics, v. 23, p. 353-411, October 1951

16. Kuhl, W., "Die Eigenschaften Wassergefüllter Rohre für Widerstands- und Schallgeschwindigkeitsmessungen," Acustica, v. 3, p. 111-123, 1953

17. Kuhl, W. and Tamm, K., "Messung der Schallausbreitung in Flüssigkeitsgefüllten Rohren mit Schallweichen Wänden," Acustica, v. 3, p. 303-316, 1953

18. Kuhl, W. and others, "Impulsverfahren zur Messung der Reflexion von Wasserschallabsorbern in Rohren," Acustica, v. 3, p. 421-433, 1953

19. Silberman, E., "Sound Velocity and Attenuation in Bubbly Mixtures Measured in Standing Wave Tubes," Acoustical Society of America. Journal, v. 29, p. 925-933, August 1957

20. Moen, C. J., "Ultrasonic Absorption in Liquids," Acoustical Society of America. Journal, v. 23, p. 62-70, January 1951

21. Knudsen, V. O., "The Effect of Humidity Upon the Absorption of Sound in a Room, and a Determination of the Coefficients of Absorption of Sound in Air," Acoustical Society of America. Journal, v. 3, p. 126-138, July 1931

22. Mulders, C. E., "Ultrasonic Reverberation Measurements in Liquids II," Applied Scientific Research, v. B1, p. 341-357, 1950

23. Ferrero, M. A. and Sacerdote, G. G., "Measurement of Acoustic Impedance in a Resonant Spherical Enclosure," Acustica, v. 8, p. 325-329, 1958

24. Karpovich, J., "Resonance Reverberation Method for Sound Absorption Measurements," Acoustical Society of America. Journal, v. 26, p. 819-823, September 1954

25. Wilson, O. B., Jr., and Leonard, R. W., "Measurements of Sound Absorption in Aqueous Salt Solutions by a Resonator Method," Acoustical Society of America. Journal, v. 26, p. 223-226, March 1954

26. Toulis, W. J., "Theory of a Resonance Method to Measure the Acoustic Properties of Sediments," Geophysics, v. 21, p. 299-304, April 1956

27. Hunt, F. V. and others, "Analysis of Sound Decay in Rectangular Rooms," Acoustical Society of America. Journal, v. 11, p. 80-94, July 1939

28. Hunt, F. V., "Notes on the Exact Equations Governing the Propagation of Sound in Fluids," Acoustical Society of America. Journal, v. 27, p. 1019-1039, November 1955

29. Morse, P. M., "Some Aspects of the Theory of Room Acoustics," Acoustical Society of America. Journal, v. 11, p. 56-66, July 1939

30. Morse, P. M. and Bolt, R. H., "Sound Waves in Rooms," Reviews of Modern Physics, v.16, p.69-150, April 1944

31. Stokes, G. G., "On the Theories of the Internal Friction of Fluids in Motion, and of the Equilibrium and Motion of Elastic Solids," p.75-129 in Mathematical and Physical Papers, v.1, Cambridge University Press, 1880

32. Rosenhead, L., "A Discussion on the First and Second Viscosities of Fluids," Royal Society of London. Proceedings, v.226A, p.1-69, 21 October 1954

33. Greenspan, M. and Tschiegg, C. E., "Effect of Dissolved Air on the Speed of Sound in Water," Acoustical Society of America. Journal, v.28, p.501, June 1956

34. Mallock, A., "The Damping of Sound by Frothy Liquids," Royal Society of London. Proceedings, v.84A, p.391-395, 15 December 1910

35. Devin, C., Jr., "Survey of Thermal, Radiation, and Viscous Damping of Pulsating Air Bubbles in Water," Acoustical Society of America. Journal, v.31, p.1654-1667, December 1959

36. Liebermann, L., "Air Bubbles in Water," Journal of Applied Physics, v.28, p.205-211, February 1957

37. Mukhopadhyay, S. K., "Ultraschallabsorption in Wasser und Ihre Abhängigkeit von Temperatur und Luftgehalt des Wassers," Acustica, v.6, p.25-34, 1956

38. Takagi, S., "Theory of the Formation of Bubbles," Journal of Applied Physics, v.24, p.1453-1462, December 1953

39. Sommerfeld , A. J. W., Mechanics of Deformable Bodies; Lectures on Theoretical Physics, v.2, Academic Press, 1950

40. LaFond, E. C., "How it Works - The NEL Oceanographic Tower," U. S. Naval Institute. Proceedings, v. 85, p. 146-148, November 1959

41. LaFond, E. C., "Oceanographic Tower," Bureau of Ships Journal, v. 9, p. 21-22, April 1960

42. Truesdale, G. A. and others, "The Solubility of Oxygen in Pure Water and Sea Water," Journal of Applied Chemistry, v. 5, p. 53-62, 1955

43. Naake, H. J. and others, "Formation of Air Bubbles in Air-Saturated Water at Reduced Pressure and Their Indication by an Acoustical Measuring Procedure," Acustica, v. 8, p. 142-152, 1958

44. Naake, H. J. and others, "Observation of the Formation and Growth of Bubbles in Water Containing Air, by Optical Methods," Acustica, v. 8, p. 193-196, 1958

45. Hsieh, D.-Y. and Plesset, M. S., "Theory of Rectified Diffusion of Mass into Gas Bubbles," Acoustical Society of America. Journal, v. 33, p. 206-215, February 1961

46. Strasberg, M., "Onset of Ultrasonic Cavitation in Tap Water," Acoustical Society of America. Journal, v. 31, p. 163-176, February 1959

47. National Research Council. Committee on Aviation Medicine. Subcommittee on Decompression Sickness, Decompression Sickness; Caisson Sickness, Diver's and Flier's Bends, and Related Syndromes, Saunders, 1951

Navy Electronics Laboratory
Report 1135

MEASUREMENT OF ATTENUATION OF LOW-FREQUENCY SOUND (5-8 KC/S) IN SMALL SAMPLES OF SEA WATER, by P. G. Hansen. 105p., 4 September 1962.

UNCLASSIFIED

Cavity resonators with acoustically soft side walls were developed for measuring sound attenuation in sea water. The equipment is capable of such measurement at discrete frequencies between 5 and 8 kc/s, in the range from 10 to 200 db/kyd. Natural sea water with suspended particulate matter and high oxygen content showed attenuations in the whole range, in contrast to either distilled or clean sea water which produced no measurable attenuation. It is suggested that fine invisible bubbles or bubble nuclei may account for the excess attenuation. Theory and experimental results are discussed fully.

1. Low frequency sound - Attenuation
2. Underwater sound - Attenuation

I. Hansen, P. G.

SR 004 03 01, Task 0580
(NEL L4-4)

This card is UNCLASSIFIED.

Navy Electronics Laboratory
Report 1135

MEASUREMENT OF ATTENUATION OF LOW-FREQUENCY SOUND (5-8 KC/S) IN SMALL SAMPLES OF SEA WATER, by P. G. Hansen. 105p., 4 September 1962.

UNCLASSIFIED

Cavity resonators with acoustically soft side walls were developed for measuring sound attenuation in sea water. The equipment is capable of such measurement at discrete frequencies between 5 and 8 kc/s, in the range from 10 to 200 db/kyd. Natural sea water with suspended particulate matter and high oxygen content showed attenuations in the whole range, in contrast to either distilled or clean sea water which produced no measurable attenuation. It is suggested that fine invisible bubbles or bubble nuclei may account for the excess attenuation. Theory and experimental results are discussed fully.

1. Low frequency sound - Attenuation
2. Underwater sound - Attenuation

I. Hansen, P. G.

SR 004 03 01, Task 0580
(NEL L4-4)

This card is UNCLASSIFIED.

Navy Electronics Laboratory
Report 1135

MEASUREMENT OF ATTENUATION OF LOW-FREQUENCY SOUND (5-8 KC/S) IN SMALL SAMPLES OF SEA WATER, by P. G. Hansen. 105p., 4 September 1962.

UNCLASSIFIED

Cavity resonators with acoustically soft side walls were developed for measuring sound attenuation in sea water. The equipment is capable of such measurement at discrete frequencies between 5 and 8 kc/s, in the range from 10 to 200 db/kyd. Natural sea water with suspended particulate matter and high oxygen content showed attenuations in the whole range, in contrast to either distilled or clean sea water which produced no measurable attenuation. It is suggested that fine invisible bubbles or bubble nuclei may account for the excess attenuation. Theory and experimental results are discussed fully.

1. Low frequency sound - Attenuation
2. Underwater sound - Attenuation

I. Hansen, P. G.

SR 004 03 01, Task 0580
(NEL L4-4)

This card is UNCLASSIFIED.

Navy Electronics Laboratory
Report 1135

MEASUREMENT OF ATTENUATION OF LOW-FREQUENCY SOUND (5-8 KC/S) IN SMALL SAMPLES OF SEA WATER, by P. G. Hansen. 105p., 4 September 1962.

UNCLASSIFIED

Cavity resonators with acoustically soft side walls were developed for measuring sound attenuation in sea water. The equipment is capable of such measurement at discrete frequencies between 5 and 8 kc/s, in the range from 10 to 200 db/kyd. Natural sea water with suspended particulate matter and high oxygen content showed attenuations in the whole range, in contrast to either distilled or clean sea water which produced no measurable attenuation. It is suggested that fine invisible bubbles or bubble nuclei may account for the excess attenuation. Theory and experimental results are discussed fully.

1. Low frequency sound - Attenuation
2. Underwater sound - Attenuation

I. Hansen, P. G.

SR 004 03 01, Task 0580
(NEL L4-4)

This card is UNCLASSIFIED.

Initial Distribution List

Bureau of Ships
Code 320 Code 370 Code 335 (3)
Code 670 Code 360 Code 688 (6)
Code 342
Bureau of Naval Weapons
DLI-3 DLI-31 (2) RUDC-11
RU-222 RUDC-2 (2) FAME-3
Chief of Naval Personnel
Tech. Library
Chief of Naval Operations
Op-07T Op-09B5 (2)
Op-03EG Op-71
Chief of Naval Research
Code 411 Code 416 Code 455
Code 461 Code 466 Code 468
Commander in Chief, PacFlt
Commander in Chief, LantFlt
Commander Operational Test and Eval. Force, LantFlt
Deputy Commander Operational Test and Eval. Force, PacFlt
Commander, Cruiser-Destroyer For, PacFlt
Commander, Destroyer For, LantFlt
Commander Submarine For, PacFlt
Commander Submarine For, LantFlt
Commander Anti-Submarine Defense For, PacFlt
Commander Training Command, PacFlt
Commander Submarine Development Group TWO
Commander Service For, PacFlt, Library
Commander Service For, LantFlt
Commander Key West Test and Eval. Det.
Naval Air Development Center, Library
Aeronautical Instrument Lab.
Naval Missile Center
Tech. Library Code 5320
Naval Ordnance Laboratory, Library (2)
Naval Ordnance Test Station, Pasadena
Annex Library
Naval Ordnance Test Station, China Lake
Tech. Director Code 753
Charleston Naval Shipyard
Portsmouth Naval Shipyard
Puget Sound Naval Shipyard
Naval Radiological Defense Laboratory
David Taylor Model Basin
Navy Mine Defense Lab., Library
Navy Training Device Center
Navy Underwater Sound Laboratory
Library (3)
ASW Tactical School, LantFlt
Naval Engineering Experiment Station
Library
Naval Research Laboratory
Library (2) Code 5120
Navy Underwater Sound Reference Lab.
Library
Air Development Squadron ONE (VX-1)
Beach Jumper Unit ONE
Beach Jumper Unit TWO
Fleet Sonar School
Fleet ASW School
Naval Underwater Ordnance Station
Library
Office of Naval Research, Pasadena
Naval Submarine Base, New London
Naval Medical Research Laboratory
Naval Personnel Research Field Activity
Washington, D. C.
Navy Hydrographic Office
Library (2)
Div. of Oceanography
Naval Postgraduate School, Library (2)
Navy Representative, Project Lincoln, MIT
Assistant SECNAV, R and D
Assistant Chief of Staff, G-2, US Army, IDB (3)
Chief of Engineers, US Army, ENGRD-MF
The Quartermaster General, US Army
R and D Div., CBR Liaison Officer
Redstone Scientific Information Center,
Redstone Arsenal
Army TRECOM, Research Reference Div.
Continental Army Command, ATDEV-8
Army Electronic Proving Ground
Tech. Library
Rome Air Development Center, RCOYL-2
Holloman Air Force Base, SRLTL
Beach Erosion Board, Corps of Engineers, US Army
Air Defense Command, AD0OA
Air University, Library AUL3T-5028
Strategic Air Command, Operations Analysis
Air Force Cambridge Laboratory CRREL-R
Headquarters, U.S. Coast Guard
Aerology & Oceanography Section
Marine Physical Laboratory, Univ. of Calif.
Scripps Institution of Oceanography, Univ. of Calif.
National Research Council
Committee on Undersea Warfare (2)
U.S. Coast & Geodetic Survey
Director, Div. of Tide & Currents
U.S. Fish & Wildlife Service, Pacific
Oceanic Fishery Investigations,
Library, Honolulu
U.S. Fish & Wildlife Service, La Jolla
South Pacific Fishery Investigations
U.S. Weather Bureau
University of Alaska, Geophysical Institute
Brown University, Research Analysis Group
University of California at Los Angeles,
Engineering Dept.
Columbia University, Hudson Labs.
Harvard University, Director, Acoustics
Research Lab.
The Johns Hopkins University
Chesapeake Bay Institute, Library
University of Miami, Marine Laboratory
University of Michigan
Great Lakes Research Division
Research Institute
New York University
Meteorology & Oceanography Dept.
A & M College of Texas, Dept. of Oceanography
Pennsylvania State University, Ordnance
Research Laboratory
University of Texas
Defense Research Laboratory
Military Physics Laboratory
University of Washington
Department of Oceanography
Applied Physics Laboratory
Yale University
Bingham Oceanographic Lab.
Lamont Geological Observatory
Woods Hole Oceanographic Institution
Laboratory of Oceanography (2)
U.S. Naval Academy
Civil Engineering Laboratory, L54
Office of Naval Research
Contract Administrator, S.E. Area
Chicago
Boston
New York
San Francisco
Allan Hancock Foundation
Arctic Research Laboratory
U.S. Geological Survey
U.S. Fish & Wildlife Service
Point Loma
Stanford
Washington, D.C. (2)
Woods Hole
Geophysics Research
Narragansett Marine Laboratory
Waterways Experiment Station
Navy Weather Research Facility
Cornell University, Dept of Conservation
Florida State University,
Oceanographic Institute
University of Hawaii, Marine Lab.
Oregon State College, Dept. of Oceanography
Rutgers University
AWS, Scott AFB, Illinois
Bureau of Comm. Fisheries, Bio. Lab.
Wash, D.C. Point Loma Sta.